

INFORMATION TO USERS

This material was produced from a microfilm copy of the original document. While the most advanced technological means to photograph and reproduce this document have been used, the quality is heavily dependent upon the quality of the original submitted.

The following explanation of techniques is provided to help you understand markings or patterns which may appear on this reproduction.

1. The sign or "target" for pages apparently lacking from the document photographed is "Missing Page(s)". If it was possible to obtain the missing page(s) or section, they are spliced into the film along with adjacent pages. This may have necessitated cutting thru an image and duplicating adjacent pages to insure you complete continuity.
2. When an image on the film is obliterated with a large round black mark, it is an indication that the photographer suspected that the copy may have moved during exposure and thus cause a blurred image. You will find a good image of the page in the adjacent frame.
3. When a map, drawing or chart, etc., was part of the material being photographed the photographer followed a definite method in "sectioning" the material. It is customary to begin photoing at the upper left hand corner of a large sheet and to continue photoing from left to right in equal sections with a small overlap. If necessary, sectioning is continued again – beginning below the first row and continuing on until complete.
4. The majority of users indicate that the textual content is of greatest value, however, a somewhat higher quality reproduction could be made from "photographs" if essential to the understanding of the dissertation. Silver prints of "photographs" may be ordered at additional charge by writing the Order Department, giving the catalog number, title, author and specific pages you wish reproduced.
5. PLEASE NOTE: Some pages may have indistinct print. Filmed as received.

Xerox University Microfilms

300 North Zeeb Road
Ann Arbor, Michigan 48106

75-25,205

BRISK, Marion Ann, 1949-
APPLICATION OF PHOTOELECTRON SPECTROSCOPY
TO SOME CHEMICAL PROBLEMS.

The City University of New York, Ph.D., 1975
Chemistry, physical

Xerox University Microfilms, Ann Arbor, Michigan 48106

© 1975

MARION ANN BRISK

ALL RIGHTS RESERVED

APPLICATION OF PHOTOELECTRON SPECTROSCOPY
TO SOME CHEMICAL PROBLEMS

by

MARION A. BRISK

A dissertation submitted to the Graduate
Faculty in Chemistry in partial fulfillment
of the requirements for the degree of Doctor
of Philosophy, The City University of New York.

1975

This manuscript has been read and accepted for the Graduate Faculty in Chemistry in satisfaction of the dissertation requirement for the degree of Doctor of Philosophy.

4-27-75
date

Arthur D. Baker
Chairman of Examining Committee

5/27/75
date

Leonard H. Schwartz
Executive Officer

Dr. R. Kirby
Dr. R. Engel
Dr. D. Beveridge
Dr. C. Dillard
Supervisory Committee

The City University of New York

Abstract

APPLICATION OF PHOTOELECTRON SPECTROSCOPY
TO SOME CHEMICAL PROBLEMS

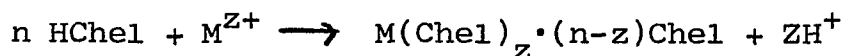
by

Marion A. Brisk

Adviser: Professor A. D. Baker

The technique of Photoelectron Spectroscopy, has already been applied to all of the major fields of chemistry, and has made valuable contributions to each of these areas. However, the potential applications of Photoelectron Spectroscopy are enormous, and a large number of investigations must be conducted before the full value of the technique can be appreciated. I have directed my thesis work to this end. Specifically, I have employed Photoelectron Spectroscopy in dealing with particular chemical problems to establish new avenues of application. In addition, specific aspects of the technique are reported which increase the information content of ESCA data.

It has long been known that many metals form adduct type complexes according to the formula:



where M is the metal and Chel is the chelating ligand in the complex. The nature of the bonding of the "extra" molecule(s)

in these adduct complexes has been the subject of many investigations. Consequently, ESCA is applied in this work to a study of some metal adduct complexes of 8-hydroxyquinoline and pyridine carboxylic acids to determine the usefulness of the technique in structure elucidation of these molecules.

Shake-up satellite peaks have been reported to appear in the photoelectron spectra of a variety of compounds ranging from rare gases to lanthanide complexes. These bands have been attributed to various mechanisms. A review of the literature indicates that the "sudden approximation" consistently explains observed satellite structure in core electron spectra. In addition, the theory attributes the observed satellite structure in transition metal core electron spectra to a charge-transfer transition. This charge-transfer process is also supported by data reported in this work involving some manganese and acetyl acetonate complexes. It is also shown that satellite intensities and positions are functions of the nature of the ligands and metal and the geometry of the complex. From this knowledge it is apparent that satellite band analysis can be used in problems involving structure elucidation of transition metal complexes.

Photoelectron spectra of some biologically important substances such as the ferridoxins has already been reported. The technique in general has been shown to be particularly amenable to proteins. In this work, ESCA is applied to some vital biochemical problems involving the structure of

cytochrome c and some copper enzymes. The results indicate that XPS can be used to determine the integrity of the Fe-S bond in many heme proteins. At this time, no other technique is capable of directly determining this information. Copper proteins have presented problems to biochemists because of the difficulty in establishing the oxidation state of the copper. ESCA however has been shown to be capable of determining the oxidation state of copper in inorganic complexes. The results of the application of the technique to tyrosinase and ceruloplasmin are reported in this work.

The last part of this thesis describes work involving VUV Photoelectron Spectroscopy. Measured ionization potentials of the "lone pair" S 3p electrons in some volatile disulfides are used to determine the dihedral angles in these molecules.

Acknowledgements

At this point I feel I should thank those people that have contributed to my educational achievements. I am most grateful to my parents for all of their help and support during all my years of education. To my mother I am particularly grateful for her unending patience, understanding and sympathy when needed. To my father I would like to express my appreciation for his deviation from the existing social institutions which permitted him "to wash the dishes and laundry while I studied mathematics." In addition, I am grateful to both of them for their expressed pride and faith in me which has been an inspiration during all of my school years. In essence, I thank my parents for living the years with me, minimizing the failures and inflating the successes.

It is also appropriate at this time to thank my mentor, Dave Baker, for making my graduate career for the most part an interesting and pleasurable experience. I feel Dr. Baker has come as close as one can to being a perfect mentor. He has always encouraged original thought and yet at the same time made sure I kept on the right track. In addition, I am grateful to him for transmitting to me some of his enthusiasm and for being the patient, kind and considerate human being that he is.

Finally, I would like to thank my closest friend Linda, for the support and encouragement she has given me during the last years of my graduate work. I am also grateful to her for reminding me through her own efforts to earn a degree, the value of an education, and for inadvertently making me realize the good fortune I have had in being able to continue my education uninterrupted with the support and love of many people behind me. Her love for life and learning are closely intermingled and knowing her has enhanced my respect for the educational process.

TABLE OF CONTENTS

CHAPTER		Page
	INTRODUCTION	1
I	INVESTIGATIONS OF SOME ADDUCT COMPLEXES .	22
	Part 1. Silver Complexes of 8-Hydroxy- quinoline and Pyridine Carboxylic Acids	26
	Part 2. A Study of the Alkali Metal Oxinate Adducts	49
	Part 3. Infrared and ESCA Studies of Some Mixed Chelate Complexes of Uranium	57
II	SHAKE-UP SATELLITE PEAKS IN PHOTOELECTRON SPECTROSCOPY	63
	Part 1. General Review	64
	Part 2. Satellite Peaks in Mn(II) Core Electron Spectra	88
	Part 3. Correlations Between a) Geometry of the Complex and Satellite Structure, and b) Between Satellite Splittings and Energies of U.V. Charge-transfer Bands	90
III	XPS OF CYTOCHROME C AND OF SOME COPPER PROTEINS	115
IV	PHOTOELECTRON SPECTRA AND DIHEDRAL ANGLES OF DISULFIDES	124

LIST OF TABLES

Table		Page
1.1	Elemental Analysis of Yellow and Green Silver Oxinates	42
1.2	Binding Energies of Various Electrons Measured With Different Spectrometers..	43-4
1.3	ESCA Results for Some Alkali Metal Complexes	56
1.4	Summary of I. R. and ESCA Values for Uranyl Complexes	60
2.1	Calculated and Experimental Satellite States in the Ne1s Photoelectron Spectrum	86
2.2	Shake-Up Probabilities For CO, CO ₂ , & C ₃ O ₂	87
2.3	Satellite Intensities in the Tetrahedral and Octahedral Chloride Complexes . . .	100
2.4	Comparison of U.V. and ESCA Data for the Lt ₂ → Mt ₂ Transition	101
2.5	Comparison of the Optical Charge-Transfer Energies and the Satellite-Main Peak Splittings	102
4.1	Ionization Potentials for Some Disulfides	126
4.2	Dihedral Angles of Disulfides Studied . .	126

LIST OF FIGURES

Figure		Page
1.	Basic Components of a Photoelectron Spectrometer	18
2.	Hewlett-Packard ESCA Spectrometer	19
3.	McPherson ESCA Spectrometer	20
4.	Structures of the Normal and Adduct Uranyl Complexes of 8-Hydroxyquinoline	25
5.	Infrared Spectra of the Yellow and Green Forms of Silver Oxinate	45
6.	The U.V. Spectrum of a Chloroform Solution of Yellow Silver Oxinate, Taken After Indicated Time Lapses	46
7.	a) I.R. and b) U.V. Spectra of Yellow Silver Oxinates Prepared in Various Solvent Systems	47-8
8.	Niels Photoelectron Spectrum Showing Main Peak and Shake-Up Satellites Only	103
9.	Some Core and Valence Electron Spectra of Ar, Kr, and Xe	104
10.	Configuration-Interaction Satellites of the Rb4s and K3s Photoelectron Spectra	105
11.	C 1s Spectra of Furan and Its Alkyl Derivative Tetrahydrofuran	106
12.	Mn2p Photoelectron Spectra of Some Mn(II) Complexes	107
13.	Cu2p XPS of CuCl and CuCl ₂	108
14.	La3d Spectra of LaF ₃ and La ₂ O ₃	109
15.	U4f _{5/2} Electron Spectrum of UO ₂ (pic) ₂ ·Hpic	110

INTRODUCTION

At the time of the writing of this thesis x-ray and vacuum ultra-violet (vuv) photoelectron spectroscopy have been shown to be of aid to the physical (theoretical and experimental), analytical, inorganic, and organic chemist as well as to the biochemist.¹ The literature attests to the fact that ESCA and PES have made considerable contributions to all of these fields. The foregoing pages will describe results from the application of ESCA and PES to structure elucidation of some organic, inorganic as well as some biochemically important compounds. Some of this work opens up new avenues of application. In addition, correlations are made between some of the ESCA data and i.r. and u. v. results.

Because of the varied nature of this research each chapter will cover a specific area of study and will contain therein all of the necessary background information which will facilitate understanding of the results. Therefore, since each chapter will have more or less its own introduction, this introduction will concentrate on a generalized discussion of the ESCA and PES technique itself, and a brief description of the photoelectron spectrometers used in this research.

If soft x-ray photons or vacuum u. v. photons impinge upon

a molecule, electrons can be ejected. The kinetic energies of these photoejected electrons are determined as a first order approximation by the well known Einstein relation,

$$\text{K.E.} = h\nu - \text{B.E.}$$

where K.E. is the kinetic energy of the ejected electrons, h is Planck's constant, ν is the frequency of the light quantum, and B.E. is the binding energy of the electrons in the sample. In photoelectron spectroscopy if the sample is irradiated with x-ray photons, the technique is generally referred to as ESCA (Electron Spectroscopy for Chemical Analysis) or XPS (X-ray Photoelectron Spectroscopy). Typical photon sources are $\text{MgK}\alpha$ and $\text{AlK}\alpha$ lines which have energies of 1253.6 eV and 1486.6 eV respectively. If vuv light is the exciting source then the technique is called VUV PES (Vacuum Ultra-Violet Photoelectron Spectroscopy) or UPS (Ultra-Violet Photoelectron Spectroscopy). The most widely used photon source in this technique is the He(I) resonance line with an energy of 21.21 eV (584 \AA). This line constitutes approximately 98% of the emission in this energy region. Resonance lines of other elements have been used by simply mixing a small amount of the desired element into the He flow. In this matter the Lyman α line ($h\nu = 10.20 \text{ eV}$) of atomic hydrogen and the Ar line ($h\nu = 11.62 \text{ eV}$) for example can be used. However other resonance lines are emitted from these

atoms at energies nearby, making the He(I) line the most widely used exciting source.

From the Einstein relation, it is apparent that by knowing the energy of the ionizing source and the kinetic energies of the ejected electrons binding energies can be obtained. Figure 1. shows schematically how a photoelectron spectrometer records binding energies of electrons in molecules. X-ray or u.v. photons are directed into the target chamber containing the sample typically in the form of a solid or gas. (Siegbahn et al. have recently developed an ESCA spectrometer which can be used for analysis of liquids.² ESCA of liquids however is a technique which is still in its early stages and consequently not much work has been reported.) After the ionizing photons impinge upon the sample, electrons can be ejected from any orbital which has a characteristic binding energy equal to, or less than the energy of the impacting photon. Binding energies of the K shell electrons for the first 18 elements range from 14-3203 eV. Valence shell electrons generally show a binding energy of somewhere between 5-30 eV. Therefore, XPS can be used to measure the binding energies of both core and valence electrons, while PES is restricted to valence electrons of molecules. The photoejected electrons pass through an exit slit into an energy analyzer.

There are various types of energy analyzers³ all of which essentially separate electrons according to their kinetic

energies. The main two classes of energy analyzers are the electrostatic deflection type and the magnetic focussing type analyzer. The Perkin Elmer PES (PS18) used in this research employs a 127° sector cylindrical electrostatic deflection type analyzer. Electrons are separated according to their kinetic energies by varying the potential between the analyzer plates. Ideally, for any one voltage value applied across the analyzer plates, electrons possessing a particular kinetic energy will be focussed on the exit slit and be counted. This approximately monoenergetic electron current is then amplified by some type of electron multiplier. These multipliers vary from the "venetian-blind" type to the very sophisticated channel multipliers or channeltrons. Gains of up to 10^9 are possible in this later type of multiplier. Channeltrons are used in the commercial ESCA spectrometers employed in this research. The counting equipment in these photoelectron spectrometers vary depending on the manufacturer. This equipment will be described briefly, later in this work. The counting equipment contained in the PS18 is standard: preamplifier, EHT, rate meter and recorder.

PES spectra were obtained when the recorder which drives the sweep voltage was set at an ionization potential of 6 eV and allowed to scan up to 21.21 eV. The spectra were therefore plotted as binding energy (x axis) versus electron count rate (y axis). ESCA spectra were acquired by setting the instrument to scan a specific energy region e.g. N 1s

390-410 eV. Consequently all electrons having an energy between $h\nu-390$ and $h\nu-410$ eV would be focussed on the exit slit and be counted. Spectra in ESCA plot count rate versus binding energy as well.

Both the ESCA and PES spectrometers require differential pumping. The analyzer and electron multiplier in the PES are maintained at a pressure of $\sim 10^{-5}$ torr while the sample vapor pressure in the target chamber is usually a few tenths of a torr. Sample vapor is continually introduced into the ionization chamber during the measurement of a spectrum since it leaks into the analyzer compartment and is consequently pumped out by the diffusion pump. The electron multiplier must be kept under a low pressure in order to avoid sparking.

The pressure in the target chamber of an ESCA spectrometer is in general much lower than that in a vuv photoelectron spectrometer. This is a consequence of the fact that ESCA is sensitive to only the surfaces of solids and any impurities such as adsorbed gases can prevent analysis of the sample. It is believed that only the first $10-20\text{\AA}$ of the sample surface can contribute photoelectrons to the electron peaks. Consequently, the pressure in the target chamber is $\sim 10^{-7}$ or 10^{-6} torr, while the analyzer and counting equipment are under an even lower pressure.

The commercial ESCA spectrometers we used in this research (Hewlett-Packard, McPherson, Dupont, Varian, AEI) displayed various resolving powers and data handling

techniques. Each instrument had its own set of advantages and disadvantages.

The Hewlett-Packard by far is the most sophisticated of the commercial spectrometers. It offers the best resolution obtainable at this time; the measured full linewidth at half maximum height (FWHM) of the C 1s peak in graphite is .75 eV, the $2p_{1/2}$, $2p_{3/2}$ levels of Si give rise to a FWHM value of .5 eV, while the corresponding width for the $4f_{5/2,7/2}$ lines of Au are .5 eV. This superior resolution is a consequence of the crystal monochromatization of the AlK α x-rays and dispersion compensation. The monochromatization results in a loss of intensity which is compensated for by a large multidetector system which increases the speed of information by a factor of more than a 100.

According to Siegbahn et al.,⁴ the H. P. Spectrometer consists of four basic components; a crystal monochromator, electron lens, the electron spectrometer (hemispherical electrostatic analyzer), and the multichannel detection system. The monochromator consist of a bent crystal which disperses the AlK α line and focusses it onto a curved crystal which is situated on an arc of the Rowland circle (Fig. 2). This crystal then focusses the photons onto the sample. Since the energy of the incident photons vary by about 1 eV, (natural linewidth of the AlK α line) the photoelectrons emanating from the particular energy level will vary also by 1 eV. The photoelectrons are then focussed onto the entrance

aperture of the hemispherical analyzer by an electrostatic lens system. The lens system also decreases the kinetic energy of the electrons to about 115eV. The voltage on the analyzer plates is set so as to pass electrons possessing an energy of between 110-120eV. Parallel lines are formed by the passed electrons on the exit plane of the energy analyzer. Each of these lines corresponds to an energy level of the sample. Although as already indicated there is a 1eV spread among the photoelectrons ejected from a particular energy level, this spread does not contribute to the width of these parallel lines. This is accomplished by the lens system, which disperses the photoelectrons so as to cancel the dispersion of the x-rays by the crystal monochromator, giving rise to the term dispersion compensation. The energy analyzer then brings those photoelectrons which have the same binding energies together to form a line at the exit plane.

A multichannel electron multiplier detects the lines of electrons within a 10eV range. The multiplier sends an amplified pulse to the output side for every incident electron. The electrons are then accelerated onto a phosphor screen giving rise to light pulses which are detected by the photosensitive layer of a Vidicon camera. This surface transforms the light pulses into electrical charges, which are stored until the electron beam of the camera scans across and converts them into electrical pulses at the output. The

signals are then transferred to the core memory of a multi-channel analyzer. The analyzer also functions to set the scan voltage of the Vidicon camera so that it can sort the incoming pulses into 128 memory channels according to the energies of the electrons. By simultaneously detecting electrons within a 10eV range, and storing them in 128 channels, the rate of data acquisition as compared to detection systems employing a single slit and multiplier giving similar resolution is 128 times faster. In addition by successive scanning, data is accumulated and stored, so that highly resolved spectra can be obtained, and substances in low concentration can be detected.

The dispersion compensated ESCA spectrometer is superior to other spectrometers since it affords higher resolution, freedom from satellites resulting from the presence of other lines in the ionizing source, and a reduced background. The latter asset increases the information content of the spectra since peaks are not as affected by instrumental shape.

The McPherson ESCA 36 used in this research does not use a monochromator or the dispersion compensation principle, but employs the usual slit system. The electron multiplier or channeltron in this case however, passes signals to a FDP 8 Minicomputer (Fig. 3). Consequently it is possible to load eight samples onto the probe at one time (H.P. takes three at once), program the computer to scan each sample a designated number of times, and to have the spectra stored

in designated memory locations. Recently, a peak deconvolution program has been incorporated into the minicomputer so that peaks arising from inequivalent atoms can be detected. A large cathode ray tube which can display the spectrum during the scanning process as well as the deconvoluted final spectra is included in both the McPherson and Hewlett-Packard instrument. The FWHM of the Au 4f line is advertised to be 1.0 eV at best, as compared to the corresponding value of 0.5 attainable on the H.P. spectrometer.

The Varian, AEI, and Dupont spectrometers have conventional systems and cannot accumulate points from repetitive scanning. The sensitivity and resolution of the instrument can be improved only by increasing the RC constant on the ratemeter and slowing down the recorder or sweep rate. Consequently, peaks observed on these spectrometers are typically broad and low intensity peaks are difficult to detect.

Two of the most controversial and in addition most troublesome features of ESCA at this time are calibration and sampling techniques. Calibration procedures have to be used in order to determine absolute binding energies from the peaks in a spectrum. Generally the peaks are calibrated against a standard calibration line. Another method of calibration which is finding a considerable degree of support, in one in which the vacuum level of the sample is located,

and all lines are calibrated relative to this level. Both of these methods will be elaborated upon in some detail below.

The C 1s line originating from the hydrocarbon contamination in the spectrometer has been used with reported success by a number of laboratories.⁵ Objections however have been raised since the source of contamination is not completely understood. The C 1s line from graphite mixed with the sample has served as a popular calibration technique. Johansson et al. however have shown this method to be reliable only under certain circumstances which will be described later.⁶ The C 1s line arising from adhesive tape, which is used as a sample backing, is extremely unreliable when the sample is an insulator. In addition to these problems the literature has complicated the matter even further by presenting various binding energy values for the C 1s line itself, thereby making direct comparisons of binding energies of sample impossible. In addition, if the sample contains carbon the validity of this calibration technique is dubious.

Several other electron lines have been used for calibration such as the Au 4f line.⁷ These peaks are narrow and intense and consequently their binding energy can readily be determined. In addition, gold is a relatively inert element thereby decreasing the chance of a reaction between the sample and the calibrant. The gold lines have been

obtained from a gold sample backing or from a gold layer which has been evaporated onto the surface of the sample. It has recently been shown however that this method is effective only under certain conditions.⁸ Broadening of the peaks have also been reported indicating the possibility of a reaction.⁹ As in the case of the C 1s line, several different binding energies have been used for the gold peaks.

In several investigations intra-sample methods of calibration have been used. For example, Cook et al.¹⁰ used the C 1s line of the triphenyl phosphine ligand to calibrate the Pt 4f_{7/2} level, as well as other core levels in a series of complexes. Intra-molecular standards however can be dangerous since a change of a substituent may affect the electron density around the element which is being used as a standard, thus rendering the calibration technique invalid. A more common intra-sample technique involves the practice of mixing a sample with a calibrant such as KCl, PbO, MoO₂, graphite as already mentioned, and LiF.¹¹ It is not clear at this point to which if any of these calibrants can provide an accurate method of standardization. The literature both supports these methods and negates them. It appears that they are primarily useful when one is dealing with a sample which is a conductor.

The main reason for all of these difficulties in calibration is sample charging. When electrons are photo-ejected from the surface of an insulator a net positive

charge is created which will have the effect of decreasing the kinetic energy of these ejected electrons. Conducting samples which are in electrical contact with a grounded source holder do not suffer from charging since secondary electrons neutralize the positive holes. Charging effects can range from less than 1eV to several electron volts. The magnitude of charging appears to be a function of the non-conducting character of the compound, the sample preparation technique, and the type of instrument employed. The assumption that is made when a standard such as a hydrocarbon or gold layer is used is that the sample surface which is emitting electrons is at the same potential as the calibrant. Johansson et al.⁶ indicate that this is the case when gold is evaporated onto the surface in the form of a spot.

We have noted in the course of our work that the degree of charging is related to the thickness of the sample: the thicker the sample the greater the charging. Johansson et al.⁶ also point out this relationship. Consequently, one can reduce this troublesome charging effect by applying the sample to the sample backing as a thin film. This can be accomplished by simply dissolving the sample under investigation in the proper solvent. The solvent should preferably be one with a high vapor pressure at room temperature.

The backing material also has a distinct effect on surface charging. Aluminum, for example, has been shown

to give rise to a greater amount of charging than gold.⁶ Adhesive tape has been reported to show random shifts. We have run the same compound using different backings and consequently have seen varying binding energies. Johansson has shown that graphite mixed with the sample is an accurate calibrant as long as the mixture is compressed and a conducting background is used.⁶ One must be very careful at times in selecting a sample backing because of the possibility of a reaction occurring. For example, we noted that on one occasion the F 1s spectrum of AgF₂ actually was distorted into a doublet when the sample was mounted on tape (the expected singlet was observed when gold served as the substrate).

A unique method of reducing charging is one which utilizes a "Floodgun." With the Floodgun in operation, the sample surface receives $\sim 10^{-10}$ A of zero volt electrons, which should therefore dissipate any positive charge that has developed during analysis. The results of A.D. Hamer et al.¹² indicate the ability of the Floodgun to neutralize charging. The Floodgun has also been shown to eliminate the problem of differential charging. In general the effect of inhomogeneous charging domains is to broaden sample peaks. The low kinetic energy electrons of the Floodgun neutralize these areas and thus reduce the peakwidths. We have used the Floodgun while examining some alkali metal complexes (Chapter 3) on the H.P. Spectrometer. The K 2p peaks appeared at

approximately 3eV to lower binding energy of the values reported by R. Nordberg et al. for potassium. This is particularly unusual in light of the fact that the potassium in our complexes is in the +1 oxidation state. The question which comes to mind is whether this binding energy is a consequence of inaccurate calibration or if perhaps a negative charge was imposed upon the insulating sample giving rise to a lower binding energy. If this latter explanation is correct, it is obvious that the electron current impinging upon the sample from the Floodgun should be decreased. Therefore it is important to have some way of monitoring the degree of charging on the sample surface so that the electron current will just neutralize the positive charge. Hamer et al.¹² accomplished this by depositing gold on the insulator and adjusting the mean energy of the Floodgun electrons so that the binding energies of gold photoelectrons have the same values as those of the free metal. This technique resulted in the acquisition of binding energies which were reproducible and in good agreement with relevant data already available in the literature. In addition, the broad peaks typical of charged samples were changed into narrow bands when the Floodgun was adjusted properly.

Another calibrating technique consists of referencing binding energies to the vacuum level¹⁴ of the sample rather than to the Fermi level, which is actually the reference

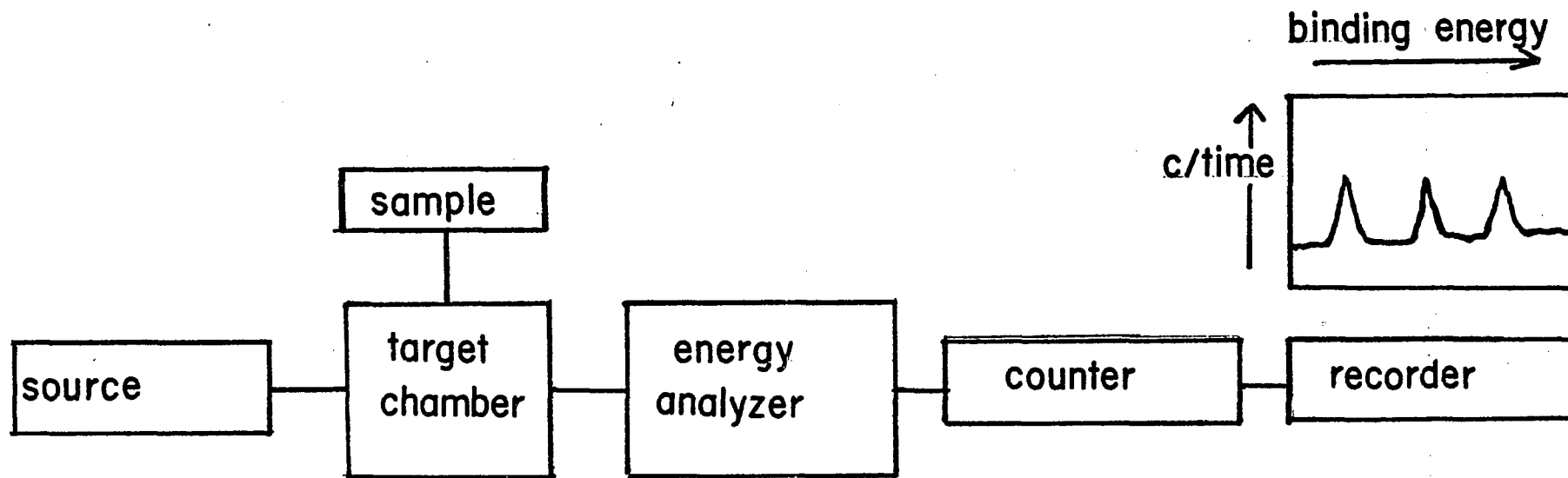
level that is used in the conventional methods already described. The assumption that is made when the conventional methods are used, is that the Fermi levels of the sample and referencing material are the same. This is true only when the sample and standard are in good electrical contact. Charging however may cause the Fermi level of the sample to drop below that of the reference making the calibration inaccurate. Vacuum level calibration avoids this problem and, in addition, affords a direct comparison between solid state and gas phase work.

The vacuum level is established by first observing the low kinetic energy onset of x-ray induced secondary electron emission of the sample. This defines the true zero of the photoelectron kinetic energy scale for the sample, since the slowest ejected electrons leave the surface with zero kinetic energy. The vacuum level therefore lies at higher kinetic energy by an amount equal to the energy of the incident photons. These slow electrons are usually detected by biasing the sample negative with respect to earth, so as to accelerate them and thus make them more easily seen on most spectrometers. The only major problem with this type of referencing appears to be the possibility of inhomogenous surface charging of an insulator.¹⁴ It is obvious that as a result of the lack of data in the literature on vacuum level calibration at this time, the validity of such a technique is dubious. At the same time, however, it offers

the possibility of eliminating the unknown factors which accompany Fermi level referencing.

It is apparent that when one is dealing with an insulator sample in general, the measurement of absolute binding energies is difficult as a consequence of the problems with calibration already described. It is also apparent that before one can be relatively sure of binding energies a number of spectra of the same energy region will have to be obtained giving rise to a consistent value. Even then values are open to criticism as a consequence of the equal Fermi level assumption which is generally made in referencing samples to standard lines. As a result of these difficulties, the binding energies determined in this research and mentioned in this work are open to question. It is interesting to note that calibration of these spectra were according to the manufacturer's suggestion. In Chapter I, the results of these suggestions will be listed. Fortunately, most of the observations and conclusions drawn are based on peak splittings or on binding energy differences between electrons emanating from the same sample, and which appear at nearby kinetic energies. The only exception to this appears in Chapter IV in which we obtained ESCA spectra of large macromolecular biochemical substances. In these cases, an intramolecular reference was used. Because of the large number of carbons in these molecules, we assumed that changing a group in the protein would not effect the C 1s line so that direct

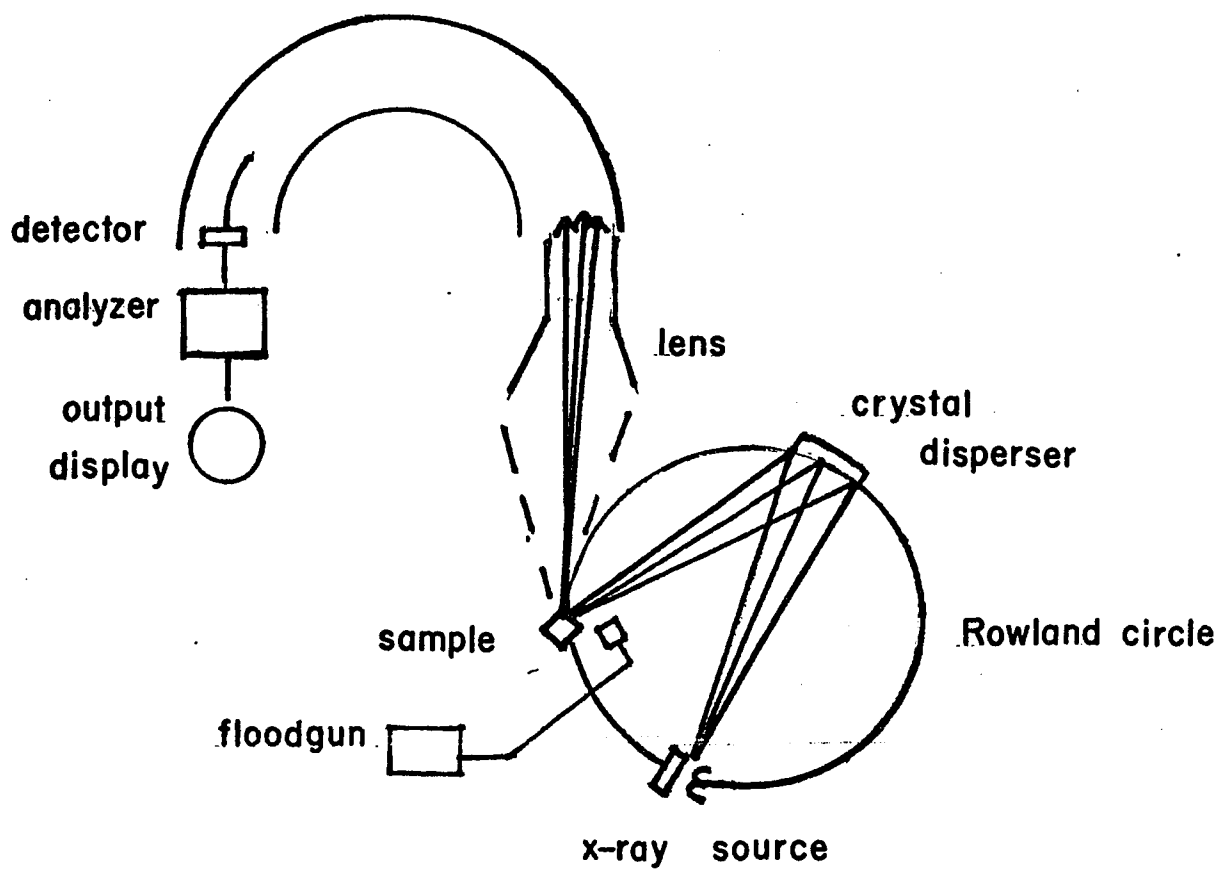
comparisons between binding energies could be made without fear of improper calibration leading to erroneous conclusions.



$$b.e. = hv - k.e.$$

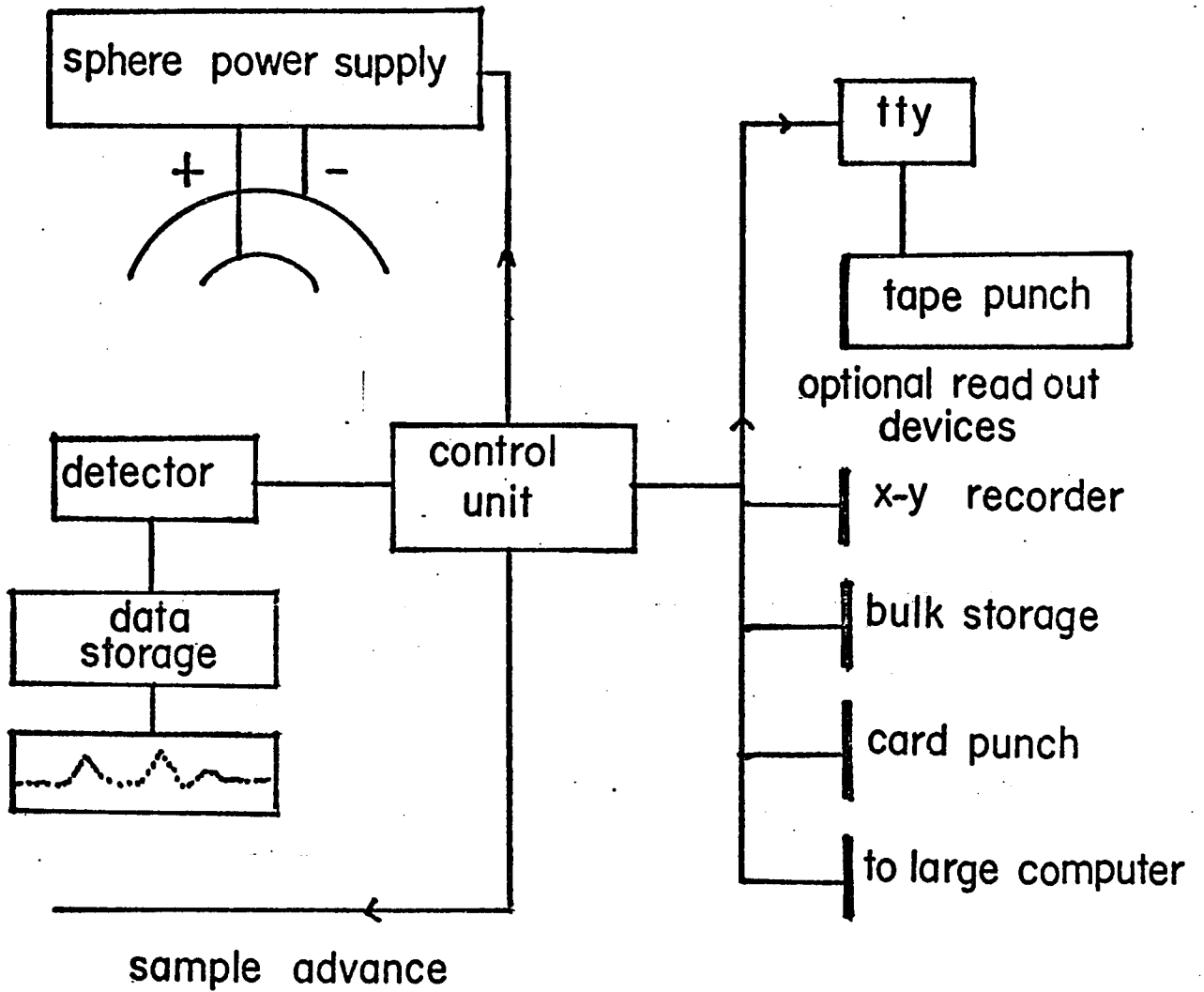
Basic Components of a Photoelectron Spectrometer

Fig 1



HP ESCA Spectrometer

Fig. 2



McPherson ESCA 36

fig 3

References

- 1 A. D. Baker and D. Betteridge, Photoelectron Spectroscopy, Pergamon Press, London, 1972.
- 2 H. Siegbahn & K. Siegbahn, J. Elec. Spectrosc., 1973, 2, 307.
- 3 K. D. Sevier, Low Energy Electron Spectrometry, Wiley-Interscience, New York, 1972, Chapters 2 & 3.
- 4 K. Siegbahn, D. Hammond, H. Fellner-Feldegg, & E. F. Barnett, Science, 1972, 245.
- 5 M. Pelavin, D. N. Hendrickson, J. M. Hollander, & W. L. Jolly, J. Chem., Phys., 1970, 74, 1116.
- 6 G. Johansson, J. Hedman, A. Berndtsson, M. Klasson, & R. Nilsson, J. Elec. Spectrosc., 1973, 2, 295.
- 7 D. J. Hnatowich, J. Hudis, M. L. Perlman, & R. C. Ragaini, J. Appl. Phys., 1971, 42, 4883.
- 8 M. V. Zeller & R. G. Hayes, J. Amer. Chem. Soc., 1973, 12, 3855.
- 9 D. Betteridge, J. C. Carver, & D. M. Hercules, 1973, 2, 327.
- 10 C. D. Cook, K. Y. Wan, U. Gelius, K. Hamrin, G. Johansson, H. Siegbahn, E. Olsson, C. Nordling, & K. Siegbahn, J. Amer. Chem. Soc., 1971, 93, 1904.
- 11 W. Bremser & F. Linneman, Chem. Ztg., 1971, 95, 1011.
- 12 A. D. Hamer, D. G. Tisley, & R. A. Walton, J. Inorg. Nucl. Chem., 1974, 36, 1771.
- 13 R. Nordberg, K. Hamrin, A. Fahlman, C. Nordling, & K. Siegbahn, Z. Phys., 1966, 192, 462.
- 14 S. Evans, Chem. Phys. Lett., 1973, 23, 134.
- 15 T. Dickinson, A. F. Povey & P. M. Sherwood, J. Electron Spectrosc., 1973, 2, 441.

CHAPTER I

Investigations of Some Adduct Complexes

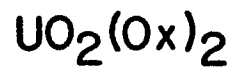
It has long been known that many metals form adduct complexes with 8-hydroxyquinoline¹ (oxine, HOx) and with some similar ligands such as the pyridine carboxylic acids.² These compounds are distinguished from the "normal" complexes in that they contain an "extra" or additional ligand molecule(s) which is either part of the coordination sphere or is a crystal-lattice component i.e. uncoordinated to the metal. The purpose of our investigations was therefore to establish the nature of the bonding of this "extra" molecule(s) in some complexes where this information had not as yet been determined. The oxinate complexes were chosen since ESCA showed itself to be a potentially useful aid in the structure elucidation of $\text{UO}_2(\text{Ox})_2 \cdot \text{HOx}$. The other adducts were studied since they form analogous complexes i.e. the same metal to ligand ratio. In all of these complexes however the coordination sites are the hard bases, nitrogen and oxygen.

Oxine is known to form two complexes with the uranyl ion; the normal chelate $\text{UO}_2(\text{Ox})_2$, which is green, and an adduct $\text{UO}_2(\text{Ox})_2 \cdot \text{HOx}$, a red compound.³ The normal chelate is prepared by heating the adduct to $\sim 210^\circ\text{C}$ for several hours.⁴ If the normal complex is then allowed to come in contact with an ethanol solution of oxine the adduct is again formed.

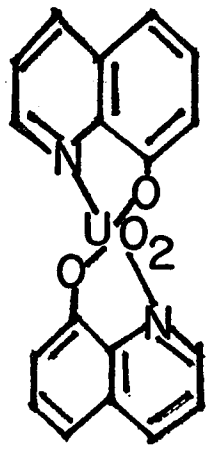
Several workers⁵ believed that the extra molecule was held by crystallization forces while others proposed that the molecule was bonded to the uranium.⁶ Infra-red data⁷ however supported the latter theory. Two broad bands appeared in the i.r. spectrum of the adduct, one at 2650cm^{-1} (medium intensity) and the other at 2050cm^{-1} (low intensity), both of which did not appear in the spectrum of the 1:2 complex. These bands were attributed to the presence of a $\text{N}^+ \text{---} \text{H} \text{---} \text{O}^-$ structure in which the first band resulted from a N-H symmetric stretch moved to lower energy by the hydrogen bond. The lower intensity absorption was assigned to a combination band between the scissoring frequency $\sim 1600\text{cm}^{-1}$ and an internal or lattice frequency $\sim 400\text{cm}^{-1}$. X-ray crystallography⁸ also supported this hydrogen bonded structure. In fact, the data indicated that two of the oxine ligands were acting as bidentates in the complex; the third ligand was bonded to the uranium through its phenolate oxygen only, while its nitrogen was hydrogen bonded to a neighboring phenolate oxygen (Fig. 4). ESCA spectra of the adduct and normal complexes agreed with the bidentate-monodentate structure.⁹ The N 1s spectrum of the adduct showed two peaks in a 2:1 intensity ratio; the more intense peak appearing at 400.5eV and the remaining at a higher binding energy of 402.5eV. The normal complex showed only one N 1s peak at 400.5eV while the analogous ESCA spectrum of oxine hydrochloride $\text{H}_2\text{Ox}^+\text{Cl}^-$ which contains a positively

charged nitrogen showed a peak at 402.1eV. It is apparent from these results that ESCA data indicates the structure as shown in Figure 4; the more intense peak in the adduct spectrum originates from the nitrogen belonging to the bidentate ligands while the peak at higher binding energy and lower intensity corresponds to the hydrogen bonded nitrogen of the monodentate oxine ligand.

Other oxinate complexes such as $\text{AgOx}\cdot\text{HOx}$ and the alkali metal complexes $\text{LiOx}\cdot\text{HOx}$, $\text{NaOx}\cdot\text{HOx}$, and $\text{KOx}\cdot\text{HOx}$ are described in the literature but without a clear indication of the nature of the bonding of the extra molecule. Consequently, we decided to investigate these oxinates hoping, of course, that application of ESCA would be of assistance as it was in the structure elucidation of the uranium oxinate adduct.

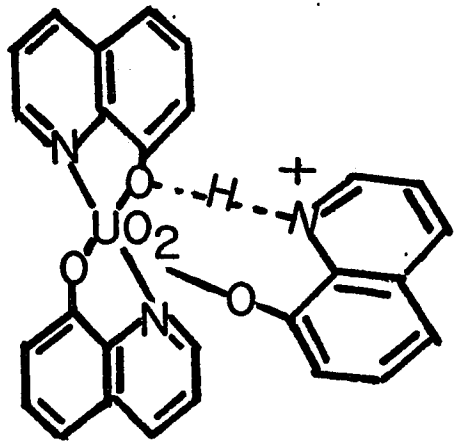


normal

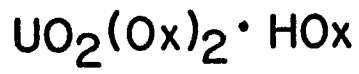


complex

adduct



complex



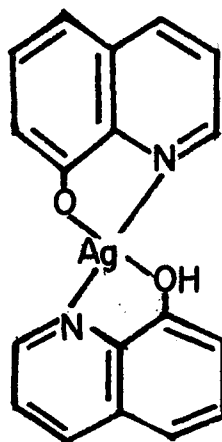
Part 1. Silver Complexes of 8-Hydroxyquinoline and Pyridine
Carboxylic Acids

Yellow and Green Forms of Silver Oxinate

When solutions of silver acetate and 8-hydroxyquinoline are mixed, either a yellow compound or a green compound is formed as a precipitate. These two compounds have been investigated previously. It was proposed that the temperature of the solutions determined which product was obtained. Early suggestions¹⁰ that the green compound contained silver (II) while the yellow contained silver (I) have been discounted on the basis of the observed diamagnetism of both.¹¹ Various observations led previous workers to conclude that the yellow and green modifications were basically identical, having the formula $\text{AgOx}\cdot\text{HOx}$, except that the green form contained some free metallic silver¹¹ presumably being formed by a partial reduction of the complex.

Attempts to remove the "extra" molecule of oxine from the complex result in total disruption of the structure.¹² No compound of the structure AgOx is known.

We now present evidence that the previously assigned structure (I) for the yellow and green silver oxinates is incompatible with some experimental observations. In addition, it appears that the yellow and green forms are in fact structurally different.



I

EXPERIMENTAL

Ultraviolet and infrared spectra were recorded on Carey 14 and Beckman IR 20 spectrometers respectively. X-ray photoelectron spectra were recorded on various instruments, spectra being calibrated and run according to the manufacturers' recommendations. Yellow and green forms of silver oxinate were prepared according to a previously described procedure involving the addition of an oxine solution to a silver acetate solution.¹³ In addition, several modifications of the yellow form were prepared by varying the solvent used to dissolve oxine before addition to the silver (I) solution.

White silver complexes of the type $\text{Ag}(\text{HOx})_2\text{X}$ ($\text{X}=\text{NO}_3$, ClO_4 , F) were prepared by following the procedure described by Hein and Regler¹⁴ for the preparation of $\text{Ag}(\text{HOx})_2\text{NO}_3$, or

by adapting it through the substitution of AgClO_4 or AgF for AgNO_3 in the synthesis.

The thermal decompositions of the latter types of complexes were studied by heating them in a vacuum sublimation apparatus at 90°C . Ag(I) and Ag(II) complexes of picolinic acid and of other pyridine carboxylic acids were prepared according to a previously described method.¹⁵ This method was further modified in that the reactants were mixed in different ratios. In one experiment AgClO_4 was used in place of AgNO_3 . Modifications of the described procedure were found to yield compounds of different compositions, as will be discussed later.

Results and Discussions

Infrared spectra of the yellow and green compounds, run as KBr pellets in the $4000\text{--}400\text{ cm}^{-1}$ region, differed significantly only in the $3000\text{--}2000\text{ cm}^{-1}$ range, where the yellow compound but not the green showed a broad but weak band at ca. 2580 cm^{-1} (Figure 5). Visible and ultra-violet spectra of the two compounds were taken in chloroform solution. The yellow compound gave a pale yellow solution, which gradually turned green. Figure 6 shows the UV and visible spectrum of a chloroform solution of the yellow compound, taken immediately, and after indicated time lapses. After 24 hours, the spectrum became identical to that of the green compound in chloroform.

Additional information about the yellow compound was acquired by changing the solvent used to dissolve oxine in its preparation.¹³ Acetone, for example, was substituted for the ethanol used in the previously published preparation. A granular yellow precipitate resulted. Since oxine is rather insoluble in water, it was not possible to prepare a yellow silver oxinate by mixing aqueous solutions of oxine and silver acetate. However, we did prepare a compound by mixing aqueous solutions of sodium oxinate 16 and silver acetate. The precipitate produced was initially yellow, but it rapidly acquired a greenish hue. Figure 7 shows the IR and UV spectra of the three yellow silver oxinates obtained from the ethanol, acetone, and water solvent systems. The UV spectra show that the relative intensities of the bands differ. In the IR spectra the main differences are in the intensities of the broad band centered at ca. 2580 cm. The intensity of this band appeared to be proportional to the "yellowness" of the compound.

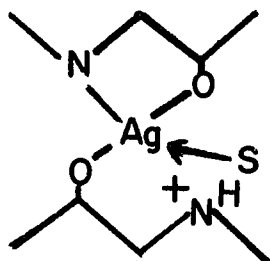
The molar absorptivity for blue light absorption (4400Å) of the yellow silver oxinate prepared using ethanol as a solvent is 3.7×10^2 , while the absorptivities for the yellow-green (H₂O used as solvent) and green modification are 1.6×10^2 and $.66 \times 10^2$ l/mole-cm respectively. The 2580 cm⁻¹ IR band of these compounds decreases in intensity in the same relative manner.

The three yellow oxinates also differ in their rates of

conversion to the green form. It has previously been reported that the yellow-to-green conversion can be brought about by heating in water. We noted that merely standing the compounds in cold water is sufficient. The rates of conversion of the different yellow silver oxinates are in decreasing order $Y_{H_2O} > Y_{EtOH} > Y_{(CH_3)_2CO}$ (Y refers to yellow silver oxinate, the subscripts refer to the solvents used in the preparations).

In order to propose an acceptable structure for the yellow silver oxinates, it is therefore necessary to take into account the different properties of the materials prepared in different solvents, and also to explain the absorption at about 2580 cm^{-1} in their IR spectra.

By analogy with the uranium-oxine adduct, it can be inferred from the IR spectra of the yellow silver oxinates that the "extra" oxine molecule in these compounds may also be monodentate, and have its nitrogen atom involved in a hydrogen bond (2580 cm^{-1} band). The presence of one bidentate and one monodentate oxine ligand would satisfy only three coordination sites of the central silver atom. We therefore propose that a solvent molecule(s) satisfies a fourth coordination site according to the structure II.



(S= Solvent Molecule)

II

In Structure II the "positive" nitrogen may be hydrogen bonded to a solvent molecule or to an adjacent ligand molecule. Such a structure would not only explain the IR spectra of the yellow silver oxinates, but would also account for the slightly different properties of the complexes prepared through the use of different solvents.

ESCA spectra were obtained for both the green and yellow modifications prepared using ethanol as the solvent. The N 1s energy region showed only one peak in both cases. We found this result surprising in light of the i.r. data which implied the presence of an N-H⁺--O structure. One can explain this result by proposing that the electron density surrounding the nitrogen in the monodentate ligand, and that in the bidentate ligand is insufficiently different to allow resolution of the peaks. An alternate explanation which is

supported by some experimental data (i.r., elemental analysis) will be offered in the following paragraph. The Ag 3d peaks of the green and yellow forms displayed the same FWHM values. This implies the incorrectness of the suggestion that the green oxinate contains free Ag as well as Ag(I). If this were the case then one would expect to see either resolved doublets or broad peaks.

In Part 3 of this chapter, we describe some work in which we compared the intensity and the absorption frequency of the N-H stretching vibration with the N 1s energy region of some adducts. It is evident from this investigation that two nitrogen ESCA peaks appear only when this i.r. band is of low frequency and medium intensity. The strength of the hydrogen bond is a measure of these two factors; the more intense and lower the absorption frequency the stronger the bond and more positive the nitrogen thus allowing the appearance of two peaks. The i.r. band of the yellow silver complex under consideration arises at 2580 cm^{-1} while the uranium oxinate complex already described shows its corresponding band at 2650 cm^{-1} . From this observation one concludes that the hydrogen bond in the former complex is stronger and therefore the band intensity should be larger. However the reverse is true, the band is hardly discernible in the silver oxinate i.r. spectrum. The conclusion to be made is that probably the amount of $\text{AgOx}\cdot\text{HOx}\cdot\text{Solvent}$ in the samples used for analysis is very small. This would account

for the ESCA results since there would only be a small amount of positively charged nitrogen, which would be difficult to detect under the large peak due to neutral nitrogen. Therefore, the yellow complex must be of somewhat intermediate composition. Elemental analysis results are reported in Table 1.1.

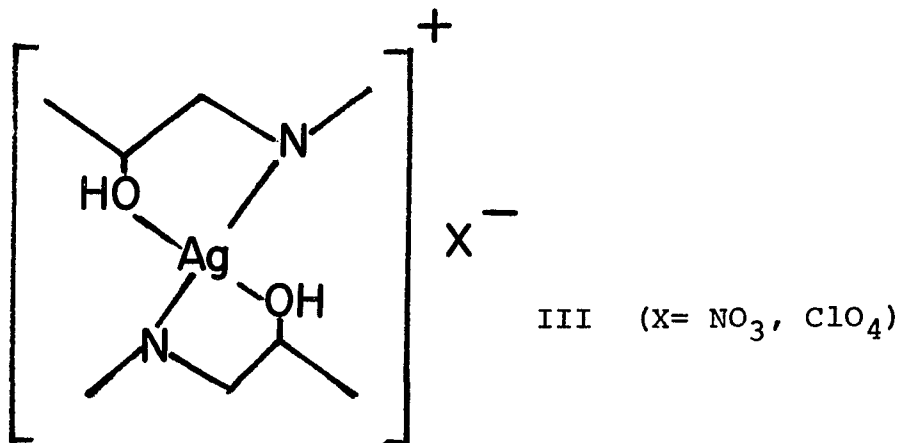
The green form of silver oxinate appears to have an appreciably lower Ag:Oxine ratio than the yellow forms. This is clear from the analysis results which show that the C, H, and N percentages in the yellow form (prepared according to reference 13) are uniformly higher than those in the green compound formed from the same solvent system at a higher temperature.

Formulae between $\text{Ag}(\text{Ox})_{1.4}$ and $\text{Ag}(\text{Ox})_{1.5}$ seem to be in best accord with the analysis results. The structural significance of this is not clear to us at this time. It is also apparent from the elemental analysis results that the whole silver/oxine system is quite complicated, and although the green form seems to differ from the yellow by virtue of lack of coordinated solvent molecule and lack of a certain fraction of the coordinated oxine molecules, it is not possible to account for this on a simple basis. Moreover, it appears that the yellow oxinates themselves cannot be assigned simple formulae. Two explanations can be advanced. Either they originally form as $\text{AgOx}\cdot\text{HOx}\cdot\text{S}$ and undergo some loss of solvent followed by perhaps co-ordinative poly-

merization during isolation, or the preparation results in a mixture of mostly $\text{AgOx}\cdot\text{HOx}$ (both ligands bidentate) and some $\text{AgOx}\cdot\text{HOx}\cdot\text{S}$ (one oxine molecule monodentate). The balance of evidence suggests the latter is more probably correct since the i.r. and u.v. experiments employed freshly prepared samples. In addition the loss of coordinated solvent and breakage of the $\text{N}^+\text{-H}\cdots\text{O}^-$ structure is a slow process as evidenced by the slow conversion of the yellow form to the green silver oxinate upon standing.

Other Silver-Oxine Complexes

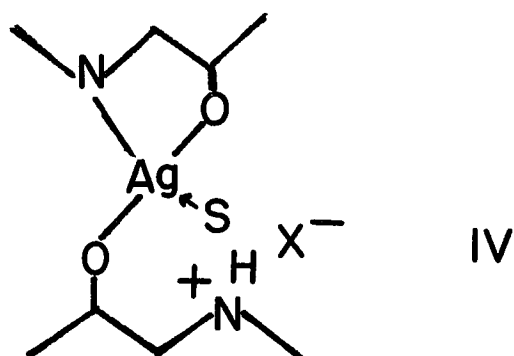
Silver has also been reported to form other types of coordination compounds with 8-hydroxyquinoline. Specifically, white compounds corresponding to the formulae $\text{Ag}(\text{HOx})_2\text{NO}_3$ and $\text{Ag}(\text{HOx})_2\text{ClO}_4$ have been described,¹⁴ and structures suggested:



In the present studies, we repeated the preparations of these compounds, and prepared $\text{Ag}(\text{HOx})_2\text{F}$ by a similar route. We also examined the thermal decomposition of the three compounds by heating them in a vacuum sublimation apparatus at 90°C . $\text{Ag}(\text{HOx})_2\text{NO}_3$ and $\text{Ag}(\text{HOx})_2\text{F}$ decomposed under these circumstances to give a yellow compound which collected around the cold finger and a dark green material which remained at the bottom of the sublimation apparatus. The yellow decomposition product of $\text{Ag}(\text{HOx})_2\text{NO}_3$ was shown to be oxine nitrate, $(\text{H}_2\text{Ox})^+(\text{NO}_3)^-$, by comparison with an authentic sample prepared by mixing dilute nitric acid and oxine. Similarly $\text{Ag}(\text{HOx})_2\text{F}$ gave $(\text{H}_2\text{Ox})^+(\text{F})^-$. The green residue remaining in each case has not been formulated as yet.

When these white complexes are stirred in water over a period of 24 hours, they are converted to a yellow silver oxinate which, in common with the other yellow silver oxinates already discussed, is converted on standing into a green form.

ESCA examination of the compounds " $\text{Ag}(\text{HOx})_2\text{X}$ " reveals a considerably broadened N 1s signal compared with that found for oxine itself. The spectra obtained point to there being two different types of ligand nitrogen atoms in a 1:1 intensity ratio. It is possible on this basis to assign a structure of the type V to the compounds, in which only one of the oxine ligands is bidentate.



Such a structure would account for the rather surprising formation of oxime nitrate on thermolysis for the nitrate complex ($V:X=NO_3$) since this would form on the breaking of the $Ag-O$ bond.

Silver Complexes with Picolinic Acid and Other
Pyridine Carboxylic Acids

Picolinic acid (HPic) and nicotinic acid (HNic) react with silver nitrate in solution to yield water insoluble white compounds, which have previously been assigned the structures $Ag(Pic)$ and $Ag(Nic)$.¹⁵ The addition of a strong oxidizing agent such as potassium persulfate to these white compounds converts them into the red $Ag(II)$ compounds $Ag(pic)_2$ and $Ag(nic)_2$, in which the geometry is tetrahedral and the ligands bidentate.

That the previously assigned formulae of the white compounds is incorrect is shown by the elemental analyses:

	<u>Silver(I) Picolinate</u>		<u>Silver(II) Picolinate</u>	
	Found	Calculated for Ag(Pic)	Found	Calculated for Ag(Pic) ₂
%Ag*	32.5	46.8	31.0	30.5
%C	32.37	31.17	40.69	40.68
%N	7.89	6.06	8.01	7.91
%H	2.32	1.73	2.44	2.26

*Determined by the Volhard method¹⁷

The IR spectra of picolinic acid and silver (I) picolinate contain similar fairly strong bands in the 2000-2600cm⁻¹ region. These bands are attributable to $\overset{+}{N}-H-\overset{-}{O}$ hydrogen bonding¹⁸ involving the carboxylic acid group and the ring nitrogen atom: they therefore indicate a -CO₂H group in the Ag(I) compound. The Ag(II) compound lacks these bands. Similar results are found from the IR spectra of nicotinic acid and of the Ag(I) and Ag(II) nicotinate.

We considered the possibility of an adduct structure of the type AgPic·HPic in the light of these results and by analogy with AgOx·HOx and with picolinic acid complexes of uranium. For example, uranium forms a 1:3 adduct UO₂(Pic)·HPic which we have found shows $\overset{+}{N}-H-\overset{-}{O}$ bonds in its IR

spectrum comparable with that in silver (I) picolinate, and which furthermore has an ESCA spectrum in accord with there being a $\overset{+}{\text{N}}\text{--H--}\overset{-}{\text{O}}$ bond in the structure.* In an attempt to discover the reason for the inexact correlation between the calculated and found percentage composition for the silver (I) picolinate, we further obtained an X-ray photoelectron spectrum of the material. When the nitrogen 1s region was scanned, two peaks appeared centered at 405.5 and 400.5 eV. The position of the higher energy peak, which appeared at approximately one-fifth the intensity of the 400.5 eV peak, correlates well with the reported binding energy value for the N 1s electrons in the nitrate anion.¹⁹ We initially considered this may be present as AgNO_3 impurity from the preparation so we repeated the preparation using a 50:1 excess of picolinic acid over silver nitrate, then repeatedly washed the product. The elemental analysis of the material obtained however, was still not in accord with the simple formula $\text{AgPic}\cdot\text{HPic}$ and the presence of nitrate was again indicated. Furthermore, mixing solutions of AgClO_4 and picolinic acid produces a white precipitate, which is shown by ESCA to contain perchlorate ion. The elemental analysis for the compounds obtained from the 50:1 picolinic acid: silver nitrate(A), and the picolinic acid: silver perchlorate (B) reactions are:

*This work is described in Part 2 of this chapter.

A: C 31.47%	N 7.62%	H 2.32%
B: C 29.82%	N 5.81%	H 2.22%

A possible explanation for these phenomena can be inferred from the corresponding silver-oxine complexes. Oxine reacts with silver nitrate and perchlorate to give $\text{Ag}(\text{HOx})_2\text{NO}_3$ and $\text{Ag}(\text{HOx})_2\text{ClO}_4$ respectively, so perhaps the corresponding picolinic acid complexes $\text{Ag}(\text{HPic})_2\text{NO}_3$ and $\text{Ag}(\text{HPic})_2\text{ClO}_4$ are formed in small quantities along with $\text{AgPic}\cdot\text{HPic}$ during the preparation of silver picolinate. Whatever the explanation, the simple formula AgPic is inappropriate, and the exact composition depends upon reaction conditions.

ESCA RESULTS

Table 1.2 gives the results of ESCA spectra of several silver compounds on different instruments using the indicated backings. It is evident that the binding energy values are not in exact agreement even after the calibration correction has been made. Where scotch tape served as a backing, measurement of the C 1s line was the calibration technique employed. The C 1s line from the compound itself was also used to calibrate spectra where metallic backings were used. All Hewlett-Packard results were calibrated in this manner. All McPherson spectra obtained using backings other than tape were calibrated by measuring separately the Au 4f line.

Upon examination of the values given in Table 2, it becomes apparent that the spectra of the Ag(I) ($\text{AgOx}\cdot\text{HOx}$) and Ag(II) ($\text{Ag}(\text{Pic})_2$) complexes showing the peaks corresponding to the silver 3d electrons indicate an expected shift when Al is used as a substrate. However, when tape or gold-plated stainless steel is employed the Ag(I) 3d electrons actually appear at slightly higher binding energies than the corresponding electrons in the Ag(II) complex. The conclusion to be made is that the Ag binding energies are not appreciably different in the Ag(I) and Ag(II) complexes and that exact calibration is quite critical and difficult using the methods employed by the instrument manufacturers on our samples.

Silver peroxide (Ag_2O_2) was examined in an attempt to see if one could measure peaks due to both Ag(I) and Ag(III) both of which are present in the compound. Only one peak due to 3d electrons appeared. The 3d binding energy values are identical in the Al and graphite runs. These values changed somewhat when tape was used as the substrate.

The AgF_2 spectra measured using different materials as backing show similar deviations. The measured silver 3d electron binding energies in AgF_2 are identical when Al or graphite are used as substrates but were different when tape served as the substrate. In addition, when the F 1s electron region was examined, the binding energy differed in all three runs. One notes the appearance of a doublet in the tape spectrum.

These observations indicate the great care which must be taken in comparing results obtained under different conditions. The practice of using the C 1s line of adhesive tape as a standard is especially suspect, because if sample themselves contain carbon, this can result in a shift in the supposed "standard" carbon peak observed and hence an error in calibration. In addition, charging effects are larger when an adhesive tape backing is employed. These difficulties are well known to specialists in ESCA and better calibrating techniques such as evaporating gold onto the substance to be examined, have been suggested, but even so recent work still indicates that even this is still a difficult technique to work with and get consistent results.²⁰ It appears that non-specialists in ESCA may encounter serious difficulties in obtaining satisfactory calibrations and results using the procedures commonly employed by ESCA companies in running spectra for customers.

Table 1.1
Elemental Analysis of Yellow and Green Silver Oxinates

Found	%C	%H	%N
(1) Yellow Silver Oxinate	54.24	3.46	7.06
(2) Green Silver Oxinate	49.07	2.93	6.36
Calculated for			
(1) AgOx·HOx	54.40	3.27	7.05
(2) Ag(Ox) _{1.4}	48.61	3.15	6.32
(3) AgOx·HOx·EtOH	54.20	4.30	6.32

Table 1.2

Binding Energies of Various Electrons Measured With Different Instruments

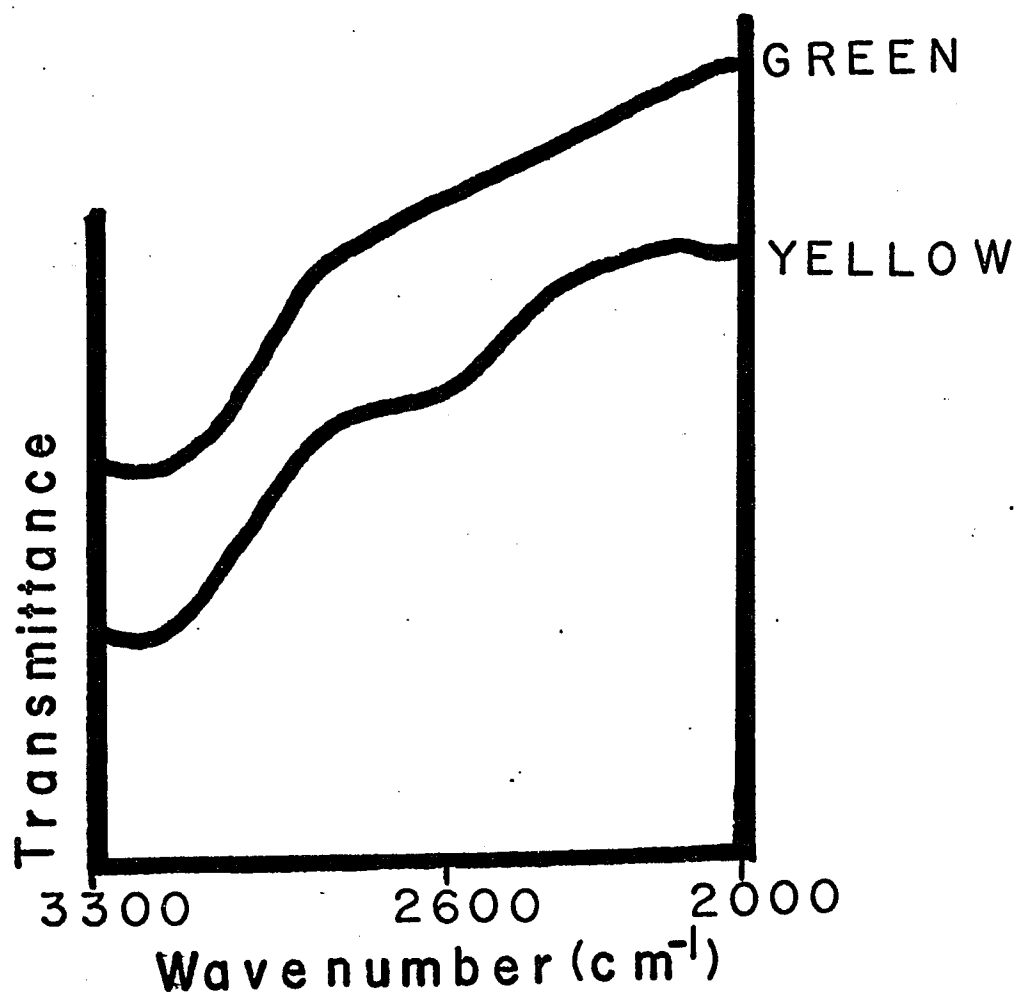
Sample	Instrument	Substrate	Ag "3d" Binding Measured (eV)	Electron Energies Corrected	N "1s" Binding Measured	Electron Energy Corrected	F "1s" Binding Measured	Electron Energy Corrected
AgOx·HOx (yellow) (green)	AEI	Tape 3d 3/2	378.1	374.2	402.3	398.4		
			372.1	368.2				
	McPherson	Al	374.5	374.8	399.6	399.9		
			368.5	368.8				
	Hewlett Packard	Au	374.5	374.2	398.3	398.0		
			368.3	368.0				
Ag(α -pic) ₂	AEI	Tape	377.8	373.9	403.4	399.5		
			371.7	367.8				
	McPherson	Al	375.1	375.4	400.5	400.8		
			369.0	369.3				
	Hewlett Packard	Au	374.8	374.0				
			368.1	367.3				

Table 1.2 Continued

Sample	Instrument	Substrate	Ag "3d" Binding Measured (eV)	Electron Energies Corrected	N "1s" Binding Measured	Electron Energy Corrected	F "1s" Binding Measured	Electron Energy Corrected
Ag ₂ O ₂	McPherson	Al	373.0	373.3				
			367.0	367.3				
		Graphite	373.0	373.3				
			367.0	367.3				
		Tape	373.6	373.9				
			367.5	367.8				
AgF ₂	McPherson	Al	373.6	373.9			686.8	687.1
			367.5	367.9				
AgF ₂	McPherson	Graphite	373.6	373.9			684.3	684.6
			367.5	367.8				
		Tape	374.7	375.0			685.7	686.0
			368.6	368.9				
Ag	McPherson		373.6	373.9				
			367.6	367.9				
UO ₂ (Ox) ₂	AEI	Au(4f _{7/2})	-----	383.2	U(4f _{7/2})	400.6		
	McPherson	Au(4f _{7/2})	-----	381.0	U(4f _{7/2})	398.5		
Ag(HOx) ₂ ClO ₂	McPherson	Al			398.8	399.1		

Fig. 5

IR Spectra of $\text{AgOx} \cdot \text{HOx}$



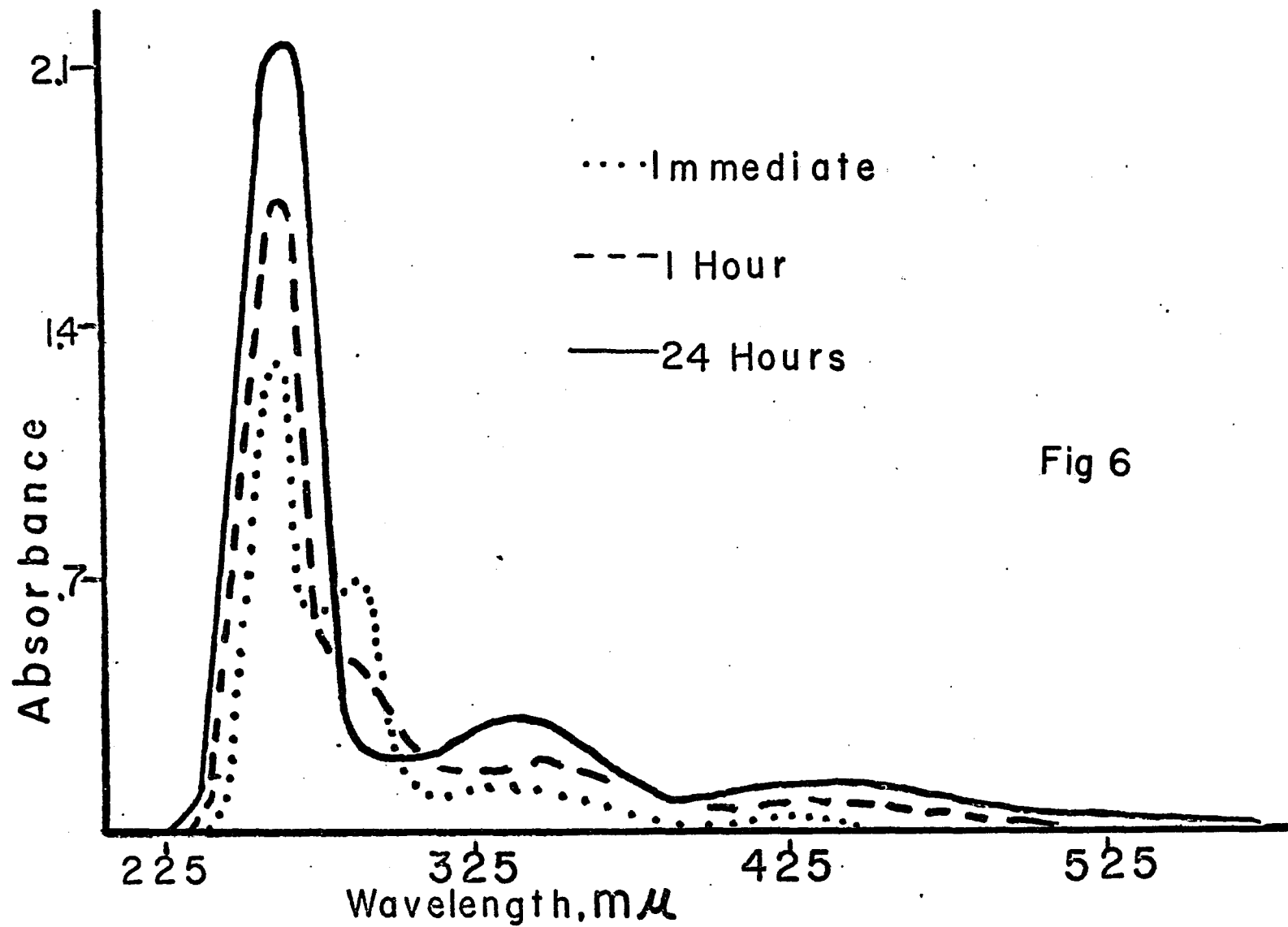
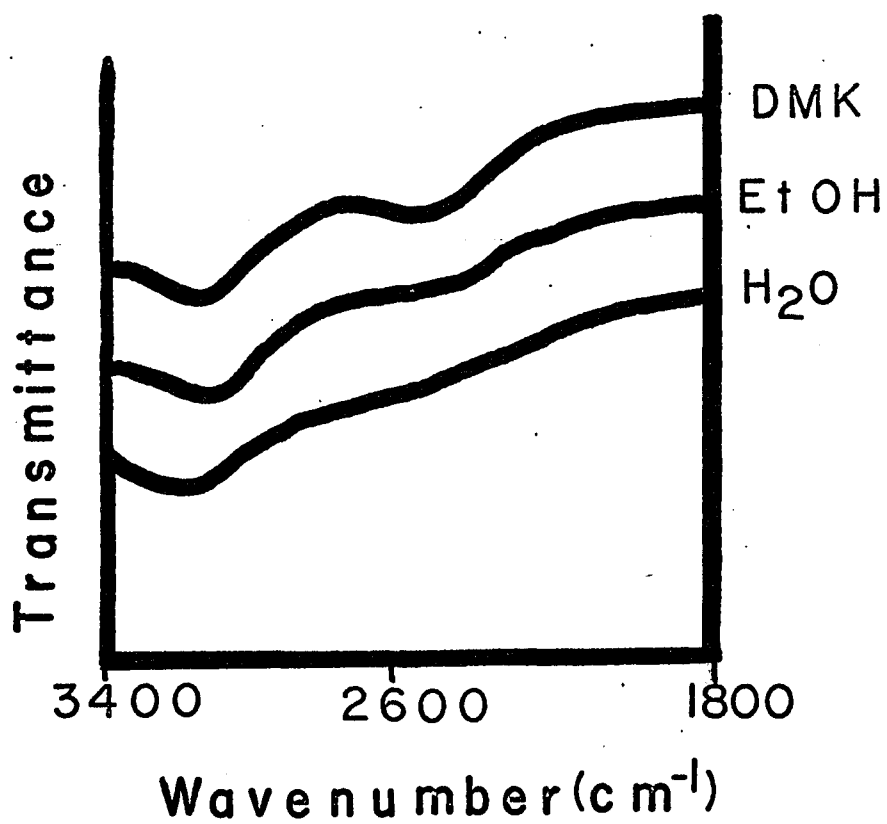
UV Spectra of $\text{AgOx} \cdot \text{HOx}$ 

Fig 7a

IR Spectra of several
modifications of silver oxinate



UV

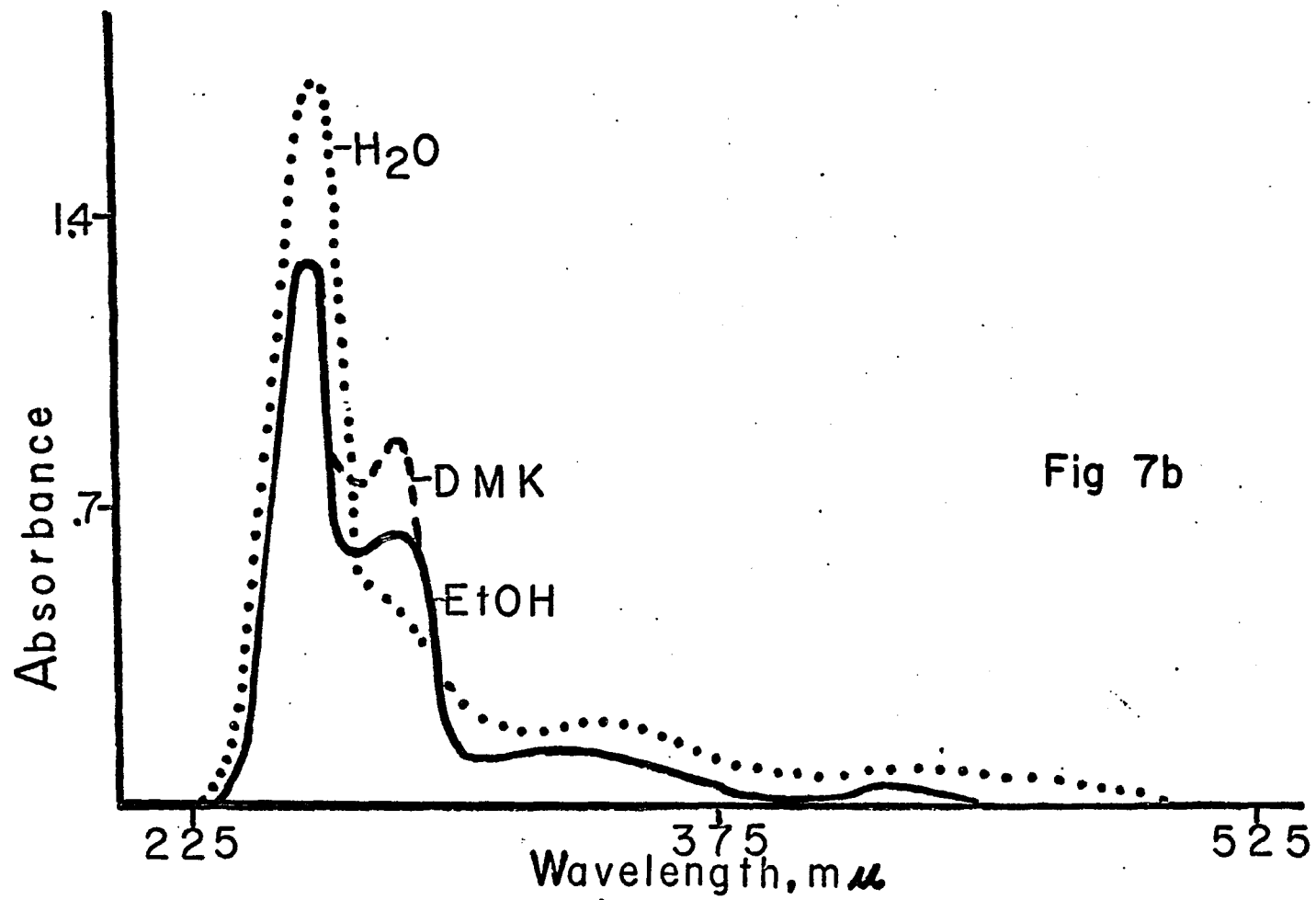
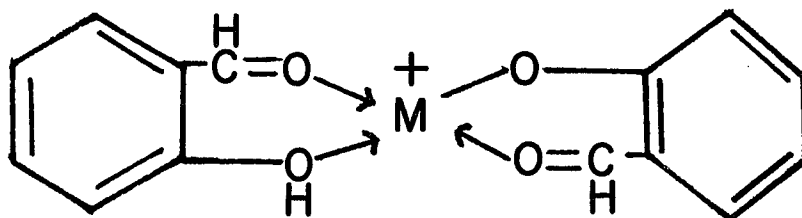


Fig 7b

Part 2. A Study of the Alkali Metal Oxinate Adducts

It is a well established fact that sodium and potassium are necessary to the normal health and growth of both plant and animal life alike. For example, it is the difference in the sodium:potassium ratio in intracellular fluids compared with the ratio in extracellular fluids that determines the various electrophysiological functions in higher animals- transmission of nerve impulses, potential across membranes and transport of ions across membranes etc. Sodium and potassium are also vital to plant metabolism. It is thought that the effectiveness of these cations is related to their ability to form complexes, although usually weak, with chelating ligands. In addition, the selectivity that is shown by various ligands for one cation over the other is also thought to be a vital factor relating to the functioning of sodium and potassium in biological systems. Consequently, it is worthwhile to investigate the structures of the complexes that sodium and potassium are known to form in general, so that perhaps trends can be observed that may relate to biological processes. In addition, the number of methods available to study the environment of bound cations are limited and it therefore may prove fruitful to apply the ESCA technique to these complexes in an effort to correlate electronic distributions with structure and perhaps stability.

Alkali metals, because of their Class A character (hard acid), are known to complex to mostly hard ligands such as O or N. Salicylaldehyde and some diketone derivatives were the first ligands to be reported which complexed with the alkali metals. Figure 8 shows the proposed structure for one of these compounds in which a ligand molecule, HL, is considered to be bound to the M^+L^- salt.



Because these adducts are soluble in nonpolar solvents, they are referred to as covalent compounds. A large number of these type of alkali metal complexes are described in the literature involving such ligands as the cyclic polyethers,²² isonitrosoacetophenone, o-nitrobenzoic acid, o-nitrophenol and anthranilic acid just to name a few.^{23,25} We decided to investigate the oxinate adducts since their structure has not been explicitly described in the literature and because of the work already done on the silver oxinates. Silver has been reported to form complexes which are similar to the alkali metal analogs.^{26,23}

EXPERIMENTAL

Ultraviolet and infrared spectra were recorded on Carey 14 and Beckman I.R. 20 spectrometers respectively. X-ray photoelectron spectra were recorded on the Hewlett-Packard 5950 ESCA spectrometer. The alkali metal complexes of 8-hydroxyquinoline and 1-nitroso-2-naphthol were prepared according to the procedure of Banerjee et al.²⁵ in which solutions of the appropriate ligand and of the appropriate metal hydroxide are combined. The thermal decompositions of the oxinate adducts were studied by heating them in a vacuum sublimation apparatus at 125 C.

Results and Discussions

The i.r. spectra of the alkali metal oxinate adducts (LiOx·HOx, NaOx·HOx, KOx·HOx) run in KBr pellets all resembled that of AgOx·HOx. A. K. Banerjee et al.²⁵ noted as we did that the 1580 cm^{-1} band of HOx is split into a higher energy band which is metal sensitive and a stationary band at 1570 cm^{-1} . In addition, however, we observed broad absorption bands of medium intensity at ~ 2560 and $\sim 2570\text{ cm}^{-1}$ in the KOx·HOx and NaOx·HOx spectra respectively, both bands of which were not noted by Banerjee et al. in their work. Consequently, we obtained spectra under the same experimental conditions as these workers i.e. samples were examined in nujol. The same bands were again observed but of much lower

intensity. Bands at ~ 1900 and ~ 1960 cm^{-1} of very low intensity also appeared in the i.r. spectra of the potassium and sodium adducts respectively.

Upon heating $\text{K}^+\text{Ox}^-\cdot\text{HOx}$ and $\text{Na}^+\text{Ox}^-\cdot\text{HOx}$ in a vacuum sublimation apparatus at 125°C , it was noted that oxine in both cases collected on the cold finger. The residue that remained after heating $\text{Na}^+\text{Ox}^-\cdot\text{HOx}$ for two hours was a yellow compound which was found to be soluble in H_2O . In addition, the I.R. spectrum of this compound revealed the absence of the bands at ~ 2570 and ~ 1960 cm^{-1} . This data adds credence to the concept that alkali metal adducts can be thought of as resulting from another ligand molecule, HL, bonding to the metal in the salt M^+L^- .

When $\text{K}^+\text{Ox}^-\cdot\text{HOx}$ is heated at 125°C for two hours, the yellow adduct turns green and then finally changes to a black-brown colored solid. This latter solid is very soluble in water giving rise to a brownish colored solution. In addition, this decomposition product is so insoluble in CHCl_3 that a spectrum could not be obtained in this solvent, although the extinction coefficients of the oxine type absorptions are usually very high ($\sim 10^5$). The I.R. spectrum of this compound indicated the presence of some form of oxine. The bands at 2560 and 1900 cm^{-1} which appeared in the I.R. spectrum of the potassium oxinate adduct were not present in the I.R. spectrum of its decomposition product.

These I.R. bands which are present in the spectra of the adducts and disappear upon heating can be assigned to an $\text{N-H}\cdots\text{O}$ structure by analogy to the work on $\text{UO}_2(\text{Ox})_2\cdot\text{HOx}$ and $\text{AgOx}\cdot\text{HOx}$. It should also be noted that the absorption bands in the $\text{KOx}\cdot\text{HOx}$ spectrum appeared to be more intense and broader than the corresponding band in the spectrum of the sodium analogue. This may indicate either a stronger hydrogen bond or that a larger number of molecules have this structure. $\text{LiOx}\cdot\text{HOx}$ did not give rise to these bands in the I.R. implying the absence of a hydrogen bonded oxine nitrogen. In addition, heating $\text{LiOx}\cdot\text{HOx}$ at 125°C did not result in decomposition. Decomposition appeared to occur at $\sim 135^\circ\text{C}$.

ESCA Results

Table 3 lists the results obtained from the HP spectrometer using gold-plated platens as a sample backing. The C 1s peak was used as a calibration line and was taken to be 285.0 eV. We feel that this calibrating technique is valid in this case since the C 1s bands arise solely from the oxine carbons which are only slightly affected by the change in metal ion. Because of the ion pumps used in the HP spectrometer, the carbon contamination layer is minimal and can be disregarded. Therefore an intramolecular standard can be used to calibrate the ESCA peaks observed. It is interesting to note that the I.R. absorption band corresponding to a C-H stretch ($\sim 3050\text{ cm}^{-1}$) appeared at almost the exact same

frequency in the spectra of these compounds.

In order to insure that the measured binding energies were not functions of the degree of charging, the samples were again mounted on the gold-plated platens but this time a gold-plated mask was placed over the sample so that only a small area of material was exposed to the x-rays. The mask, being made of a conducting substance, would help to neutralize the positive charge which develops on the surface of the sample. Consequently, the sample peaks should be shifted to lower binding energies. If the C 1s peak is an accurate calibration line then it should also be shifted to lower energy by the same amount. As it turned out this is what occurred, and therefore, the binding energies reported in Table 3 do not reflect charging effects.

The FWHM values reported in Table 3 for $\text{K}^+\text{Ox}\cdot\text{HOx}$ and $\text{Na}^+\text{Ox}\cdot\text{HOx}$, imply the existence of two inequivalent nitrogens in each of these molecules. The N 1s peaks of the adducts are decidedly broader than the corresponding peaks in the appropriate salts. This is a manifestation of the $\overset{+}{\text{N}}\text{-H}\text{-}\text{O}$ structure which was found to be present from analysis of I.R. data. In addition, the N 1s peaks of these two adducts appeared at higher binding energies as compared to the N 1s peaks of the corresponding salts. The narrow N 1s peak of $\text{Li}^+\text{Ox}\cdot\text{HOx}$ also coincides with I.R. data which indicates the absence of a $\overset{+}{\text{N}}\text{-H}\text{-}\text{O}$ structure in the molecule.

The K2p binding energies of the two potassium adduct complexes examined were lower than those of the corresponding salts. This same result can be seen for the sodium system but to a lesser degree owing perhaps to incomplete decomposition of the sodium adduct. Until now the term complex was applied to these adducts solely because they are soluble in non-polar solvents. However, our ESCA data indicates that these compounds are true complexes by virtue of the observed chemical shifts. Because binding energies are in general a function of electron density around the atom or ion under consideration, the lower binding energies in the adducts indicates a higher electron density around the metal. This in turn means that electron density is being donated to the metal at the coordination site(s).

Table 1.3

ESCA Results for Some Alkali Metal Complexes

	Binding Energies (eV)		FWHM (cm)	
	N 1s	Metal Electron	N 1s	Metal Electron
NaOx•HOx	398.7	Na2s 61.4	5 1/2	6 1/2
NaOx	397.4	61.7	3 1/2	6
KOx•HOx	398.8	K2p 291.1	5	3
KOx	396.8	291.6	2 1/2	2 1/2
LiOx•HOx	398.9		3	
KL•HL		291.0		3
KL		291.6		2 1/2

HOx = 8-Hydroxyquinoline

L = 1-Nitroso-2-Naphthol

Part 3. Infrared and ESCA Studies of Some Mixed Chelate Complexes of Uranium

A number of mono-protonated ligands (HChel) are known to react according to the following equation:



As already mentioned, when HChel=8-hydroxyquinoline, the extra molecule of ligand is bound through its phenolate oxygen while its nitrogen is hydrogen bonded to a neighboring phenolate oxygen on one of the bidentate ligands. We have prepared a number of uranyl complexes in which HChel is a pyridine carboxylic acid as well as some mixed chelate complexes. These latter adducts are synthesized by first preparing the 1:2 complex and then adding the appropriate ligand. Analysis of i.r. spectra and N 1s ESCA spectra indicated that all of the complexes prepared have a structure analogous to that of $\text{UO}_2(\text{Ox})_2 \cdot \text{HOx}$. Consequently, a correlation could be made between the strength of the hydrogen bond and the positive character of the nitrogen in that hydrogen bond. Because of the importance of hydrogen bonding in general, and the apparent lack of data concerning electron distributions in such structures, we thought that this study may be of some significance.

EXPERIMENTAL

The complexes prepared and examined in this study were $\text{UO}_2(\text{Pic})\cdot\text{HPic}$, $\text{UO}_2(\text{Nic})_2\cdot\text{HNic}$,²⁷ $\text{UO}_2(\text{Pic})_2\cdot\text{HOx}$,²⁷ $\text{UO}_2(\text{Pic})_2\cdot\text{HNic}$,²⁸ $\text{UO}_2(\text{Ox})_2\cdot\text{HPic}$,²⁷ and $\text{UO}_2(\text{Ox})_2\cdot\text{HNic}$.²⁸ The adduct complexes of picolinic and nicotinic acid were prepared according to the method of Eberle and Robel.²⁸ The mixed chelate complexes were prepared by first synthesizing the normal or 1:2 complexes and then adding it to a saturated ethanolic solution of the desired ligand. The mixed chelate precipitated almost immediately. I.R. spectra were obtained using KBr pellets on a Beckman I.R. 20 Spectrometer while the ESCA spectra were obtained from the McPherson ESCA 36. The C 1s line (285.0) was used for calibrating the spectra. As in the case of the alkali metal complexes, the narrow peaks and consistent data implied the validity of this calibration procedure.

Results and Discussions

The relevant results are reported in Table 4. As stated previously the I.R. bands have been assigned to a hydrogen bonded nitrogen system.⁷ The highest energy absorption belonging to the $\overset{+}{\text{N}}\text{--H--O}$ structure is a result of the N-H stretch (normally about 3200 cm^{-1}) being moved to a lower energy as a result of hydrogen bonding. The stronger the bond, the broader is the band and the lower the energy absorption. From Table 4 it is evident that the N 1s electron binding

energy of the "extra" ligand in different complexes increases as the strength of the hydrogen bond increases. For example, the highest energy absorption associated with $\overset{+}{N}-H-O$ bonds in $UO_2(Ox)_2 \cdot HPic$ occurs at 2400 cm^{-1} . $UO_2(Pic)_2 \cdot HPic$ absorbs at 2680 cm^{-1} . Consequently, the hydrogen bond appears to be stronger in $UO_2(Ox)_2 \cdot HPic$ and the N 1s electron binding energy of the "extra" ligand (HPic) is also higher. From this data it is apparent that the more positive the nitrogen the stronger the hydrogen bond.

Table 1.4

Summary of I. R. and ESCA Values for Compounds Studied

Compound	Absorption Associated With N--H--O Bonds (cm^{-1})	+ N 1s Electron Binding Energy (eV)
$\text{UO}_2(\text{Nic})_2 \cdot \text{HNic}$	2800 vb	403.2
$\text{UO}_2(\text{Pic})_2 \cdot \text{HNic}$	2800 m	403.0
$\text{UO}_2(\text{Ox})_2 \cdot \text{HNic}$	2800 w	402.8
$\text{UO}_2(\text{Ox})_2 \cdot \text{HPic}$	2400 vb	402.8
$\text{UO}_2(\text{Pic})_2 \cdot \text{HPic}$	2680 vb	402.6
$\text{UO}_2(\text{Ox})_2 \cdot \text{HOx}$	2650 vb ^a	402.1 ^b
$\text{UO}_2(\text{Pic})_2 \cdot \text{HOx}$	2700 vb	401.8

a Value taken from ref. 7.

b Value taken from ref. 9.

References

- 1 R. G. Charles & A. Langer, J. Phys. Chem., 1959, 63, 603.
- 2 L. J. Park, "Studies of Complexes of Pyridine Carboxylic Acids," University Microfilm, Ann Arbor Michigan, 1965.
- 3 T. Moeller and M. V. Ramaniah, J. American Chem. Soc., 1954, 76, 5251.
- 4 A. Corsini and J. Abraham, Talanta, 1968, 15, 562.
- 5 T. Moeller and M. V. Ramaniah, (a) J. Amer. Chem. Soc., 1953, 75, 3946; (b) J. H. Van Tassel and W. W. Wendtlandt, J. American Chem. Soc., 1959, 81, 813; (c) L. Pokras, M. Kilpatrick, and P. M. Bernays, J. Amer. Chem. Soc., 1953, 75, 1254.
- 6 E. P. Bullwinkel and P. Nobel, J. Amer. Chem. Soc., 1958, 80, 2955.
- 7 A. Corsini, J. Abraham, and M. Thompson, Chem. Comm., 1967, 1101; Talanta, 1971, 18, 481.
- 8 D. Hall, A. D. Rae, and T. N. Waters, Acta Cyst, 1967, 22, 258.
- 9 D. B. Adams, D. T. Clark, A. D. Baker and M. Thompson, Chem. Comm., 1971, 1600.
- 10 S. L. Tzinberg, Fact. Lab., Moscow, 1937, 6, 499.
- 11 B. P. Block, J. C. Bailar, and D. W. Pearce, J. Amer. Chem. Soc., 1951, 73, 4971.
- 12 W. W. Wendlandt, Analyt. Chem., 1956, 28, 499.
- 13 Y. Nakatsuka, Bull. Chem. Soc. Japan, 1936, 11, 45.
- 14 E. Hein and H. Regler, Chem. Ber., 1936, 69, 1692.
- 15 J. A. Azoo, R. G. Bacon, and K. K. Gupta, J. Chem. Soc. (A), 1970, 1975.
- 16 A. K. Banerjee, A. J. Layton, R. S. Nyholm, and M. R. Truter, J. Chem. Soc. (A), 1969, 2536.
- 17 R. A. Day and A. L. Underwood, Quantitative Analysis, 2nd ed., Prentice-Hall, New Jersey, 1967, Ch. 6.

- 18 R. F. Evans and W. Kynaston, J. Chem. Soc., 1962, 1005.
- 19 D. P. Murtha and R. A. Walton, Inorg. Chem., 1973, 68, 123.
- 20 M. V. Zeller and R. G. Hayes, J. Amer. Chem. Soc., 1973, 12, 3855.
- 21 J. Kleinberg, W. J. Argersinger & E. Griswald, Inorganic Chemistry, Heath, Boston, 1960, 310.
- 22 D. Bright & M. R. Truter, Nature, 1970, 225, 176.
- 23 M. R. Truter, Chemistry in Britain, 1971, 203.
- 24 A. J. Banerjee, A. J. Layton, R. S. Nyholm, & Mary R. Truter, Nature, 1968, 217, 1147.
- 25 A. K. Banarjee, A. J. Layton, R. S. Nyholm, & M. R. Truter, J. Chem. Soc. (A), 1969, 2536.
- 26 J. Barnes & C. S. Duncan, J. Chem. Soc. Dalton, 1972, 1732.
- 27 S. H. Eberle & W. Robel, Inorg. Nucl. Chem. Lett., 1968, 113.
- 28 These mixed chelates have not been reported as yet, but were prepared according to the method employed for the synthesis of $UO_2(Ox)_2 \cdot HPic$ and $UO_2(Pic)_2 \cdot HOx$. Because picolinic and nicotinic acid in general² form analogous complexes, the formulas reported appear reasonable. In addition, thermal decomposition of these mixed adducts produced the "extra" molecule as well as the normal complex.
- 29 A. D. Baker, M. Brisk, & A. Storch, J. Inorg. Nucl. Chem., 1974, 36, 1.

CHAPTER II

Shake-up Satellite Peaks in Photoelectron Spectroscopy

"Extra" peaks have been observed in the core and valence electron spectra of a wide variety of molecules. These peaks have been described as shake-up satellite peaks, and their origin has been investigated in a large number of works. Part 1 of this chapter is a review which describes and analyzes reported shake-up bands.⁶⁶ Parts 2 and 3 deal with the work we have done involving satellite structure in the core electron spectra of some transition metal complexes. Our work not only adds to existing knowledge of this phenomenon, but also, suggests possible applications of satellite peak analysis.

I. INTRODUCTION AND BASIC THEORY

A. General Comments

Shake-up satellites have been reported to appear in the x-ray photoelectron spectra of a large number of substances ranging from simple noble gas atoms¹⁻³ to rare earth^{4,5} and uranium (VI) compounds.^{5,6} The "Sudden Approximation"⁷⁻⁹ theory generally enables the nature of the valence excitation or excitations giving rise to satellite peaks to be investigated. In this review, we collect together information on satellite peaks, and describe the appropriate valence excitations as determined by the application of the Sudden Approximation and other data.

B. The Sudden Approximation

When a core electron is photoejected, the coulombic potential experienced by the outer shell electrons is suddenly altered. This sudden perturbation may induce a "shake-up" transition, involving the excitation of a valence electron to a higher, previously unoccupied orbital. The shake-up process is thought of as taking place simultaneously with the core electron photoejection.

If shake-up occurs, the kinetic energy of the ejected core electron will be less than that of an electron ejected from a corresponding core orbital in another molecule where shake-up has not occurred. Consequently, shake-up satellites

always appear on the higher binding energy side of the main peaks.

Shake-up satellites in the XPS of neon (Figure 8) have been analyzed by Siegbahn and co-workers² in terms of the Sudden Approximation. The following description and arguments are abstracted from their book "ESCA Applied to Free Molecules."

When a N particle system undergoes electron photoejection, producing an (N-1) particle system, the process is considered sudden, and analogous to the annihilation of the electron. The final state of the (N-1) particles is not an eigenstate of the new Hamiltonian but rather a linear combination of such eigenstates as represented in equation (1)

$$a_i \Psi_0(N) = \sum_f c_{if} \Psi_f(N-1)$$

where a_i is the operator annihilating an electron in state i , $\Psi_0(N)$ is the ground state determinant of the N electron system, and $\Psi_f(N-1)$ are Hartree-Fock solutions of the (N-1) electron system.

Equations (2) and (3) follow from equation (1), where P_{if} is the probability that the (N-1) electron system will be in the Ψ_f state after photoejection.

$$c_{if} = \langle \Psi_f(N-1) | a_i | \Psi_0(N) \rangle \quad (2)$$

$$P_{if} = |c_{if}|^2 = |\langle \Psi_f(N-1) | a_i | \Psi_0(N) \rangle|^2 \quad (3)$$

In order that $P_{if} \neq 0$ it is necessary that $\psi_f(N-1)$ and $\psi_0(N)$ have the same symmetry. Consequently, the monopole selection rules $\Delta J = \Delta L = \Delta S = \Delta M_j = \Delta M_s = 0$ govern shake-up in photoelectron spectroscopy. Furthermore, if the orbital approximation is applied (the total wavefunction of an atom is considered to be the product of one-electron wavefunctions), equation (4) can be introduced:

$$P_{f \leftarrow 0} = |\langle \psi_{m'l_j}(f) \psi_{m'l_j}(0) \rangle|^2 \quad (4)$$

where $\psi_{m'l_j}$ is the relaxed atomic orbital of the excited electron and $\psi_{m'l_j}$ is the atomic orbital of the electron in its ground state. $P_{f \leftarrow 0}$ is the probability that the electron in the $\psi_{m'l_j}$ ground state orbital will be found in the orbital of the ion. Therefore orbital monopole selection rules apply, viz., $\Delta j = \Delta l = \Delta m_j = \Delta m_s = 0$.

Equation (4) indicates that the electron that is excited cannot change its orbital or spin angular momentum, and thus can only change its principal quantum number, n . The value of n' will depend on the overlap integral given by equation (4).

II. OBSERVATION OF SATELLITE PEAKS

A. Noble Gases

From the selection rules for the shake-up process,

Siegbahn et al.² assigned the satellites in the neon 1s XPS spectrum to excitations of either a $2p \rightarrow n'p$ or a $2s \rightarrow n's$ type (both give rise to a 2S final state). In order to determine n , Hartree-Fock type calculations were carried out, and the excitation energies calculated. The results of the calculations consistently differed from the experimental values by about 1.8 eV--the calculated main peak-to-satellite peak splitting being too small. However, the calculated differences between the satellites themselves agreed very closely with the experimentally observed differences.

Spears, Fischbach, and Carlson examined the core and valence x-ray photoelectron spectra of argon, krypton, and xenon, as well as those of some isoelectronic alkali metal halides (see Figure 9).³ Other complementary studies on helium^{1,10-12} and neon^{2,11,13} have also been made. The following points were made by Spears et al. regarding the application of the Sudden Approximation:

- a. Equations (1)-(4) are expected to be valid only if the velocity of the photoejected electron greatly exceeds the orbital velocity of an outer shell electron. Consequently, shake-up satellite peaks arising from MgK_{α} excitation for example should be identical to the analogous peaks observed when AlK_{α} lines

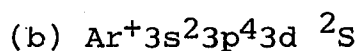
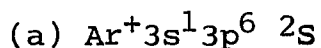
serve as the exciting source.

- b. Equation 4 implies that the probability of shake-up is not dependent on the exact core electron which is ejected since the central potential seen by the valence electrons is changed by approximately the same amount.
- c. The energy of excitation (main peak-to-satellite peak spacing) should also be independent of the core electron ejected. It should be a function of Ψ_{mlj} and $\Psi_{m'l'j}$.

Observations of satellite structure in various core photoelectron spectra, and in spectra obtained using several different impacting photon energies, substantiate the above points.

Energies of excitation, and the probabilities of the shake-up processes have been calculated using the Hartree-Fock wave-function program of Fischer.¹⁴ Good agreement between calculated and observed quantities is found (Table 2.1), providing further justification for the applicability of the Sudden Approximation. Another result to emerge from this study was that optical absorption spectra data for the excitations involved in the shake-up agreed very well with the satellite-to-main peak spacings from the XPS data.

Shake-up satellites were also reported in the valence photoelectron spectra of rare gases in addition to satellites arising from configuration interaction (two-electron excitation). An example of this latter process occurs in the 3s XPS spectrum of argon. Consider the two final states (a) and (b) for an argon ion:



The type of configuration interaction shown in state (b) is favorable since all of the orbitals involved in the process have the same principal quantum number thereby giving rise to a significant overlap between the appropriate orbitals.

B. Alkali Halides

Satellite structure was observed in the valence spectra of some alkali halides by Wertheim and Rosencwaig.¹⁵ Satellite peaks were seen associated with the Rb 4s and K3s main peaks in the halides, but not with the Na 2s main peaks (see Figure 10). The origin of the satellites was believed to lie in a configuration interaction (C.I.). This would be consistent with the vanishingly small intensity of the Na 2s satellite since the predicted position of such a C.I. satellite is $\sim 20\text{eV}$ from the main peak, and Perturbation Theory suggests that the intensity of a satellite should be inversely proportional to the separation from the main peak. In accord with this is the observation that in this study,

the satellite associated with the Rb 4s peak was the most intense satellite seen; the satellite peak appearing only about 10 eV from the main peak.

Spears et al.³ were able to make a direct comparison between satellites associated with the XPS of rare gas atoms and those associated with the isoelectronic alkali metal ions. The satellite peaks are more intense for the alkali metal ions, as shown by their XPS studies and those of Werthiem and Rosencwaig on the alkali metal halides (Figures 2 & 3). Comparisons between XPS data and optical data confirm the C.I. process.

C. Small Molecules

Aarons, Guest, and Hillier extended the Sudden Approximation to simple molecules in order to interpret observed satellite structure.¹⁶ If ψ_{mlj} and $\psi_{m'l'j}$ (equation 4) are now molecular orbitals, ψ_0 and $\psi_{f\alpha}$, for, respectively, the neutral molecule and an ion with an inner shell vacancy on an atom α , they can be expressed as linear combinations of atomic orbitals (LCAOs), as indicated in equations (5) and (6):

$$\psi_0 = \sum_{u=1}^D l_u \phi_u \quad (5)$$

$$\psi_{f\alpha} = \sum_{v=1}^N k_v \phi_v' \quad (6)$$

where n is the number of orbitals in the basis set (only valence orbitals involved), and ϕ_v' represents relaxed atomic orbitals.

Equation 7 follows from equation (4), (5), and (6):

$$P_{f\alpha \leftarrow 0} = \left| \sum_{u=1}^n \sum_{v=1}^n k_{vf} l_{u0} \langle \phi_v' | \phi_u \rangle \right|^2 \quad (7)$$

Equation (7) thus describes the probability of an electron in M.O. ψ_0 being excited to M.O. $\psi_{f\alpha}$.

Equation 7 reduces to equation 8 if the ZDO approximation is used:

$$P_{f\alpha \leftarrow 0} = \left| \sum_{u=1}^n k_{uf} l_{u0} \langle \phi_u' | \phi_u \rangle \right|^2 \quad (8)$$

Carlson, Krause and Moddeman¹¹ reported weak satellites in the C 1s and O 1s spectra of CO and CO₂. Gelius et al.¹⁷ reported comparatively intense satellite peaks in the analogous spectra of C₃O₂. Aarons et al.¹⁶ also observed satellites in these three compounds and applied the Sudden Approximation in order to determine the valence excitations giving rise to the shake-up peaks. Probabilities were calculated by obtaining wavefunctions from the INDO¹⁸ approximation. Separations of satellites from main peaks were calculated approximately by considering the excitation or transition energy ΔE :

$$\Delta E = \epsilon_{f'} - \epsilon_{i'} - J_{i'f'} + 2K_{i'f'} \quad (9)$$

These quantities are calculated for the ion.

It is obvious that the only valence transitions which can give rise to shake-up satellites in core electron spectra of CO are of a $\pi \rightarrow \pi^*$ or $\sigma \rightarrow \sigma^*$ nature. Table 2.2 shows the calculated intensities (probabilities) and energies of excitation as well as the observed values. Individual assignments to peaks could not be made because of the complex nature of the spectra.

CO₂, because of its D_{∞h} symmetry, requires an additional consideration in making peak assignments. If upon core electron ejection the ion retains the symmetry of the neutral molecule then the only transitions allowed (equation 7) are of a $u \rightarrow u^*$ or $g \rightarrow g^*$ nature. Therefore in the C 1s spectrum of CO₂, the only transition which shows any significant intensity is the $2\sigma_u \rightarrow 3\sigma_u$. When a hole is created in the O 1s level the interpretation is more complex. If the hole is considered to be delocalized over equivalent sites then retention of symmetry requires the $u \rightarrow u^*$ and $g \rightarrow g^*$ selection rules while if the hole is localized the D_{∞h} symmetry breaks down, thereby allowing otherwise forbidden transition to occur. The results of calculations in which the localized hole assumption is made attribute the highest probability to the $2\pi \rightarrow 3\pi$

transition which correlates with the $1 \pi_g \longrightarrow 2 \pi_u$ transition in the neutral molecule. Table 2 shows a good correlation between calculated and observed values lending credence to the localized hole theory.

Gelius et al.¹⁷ and Aarons et al.¹⁶ observed stronger satellite peaks in the C 1s and O 1s spectra of C_3O_2 . In the former work one of the C 1s satellites was thought to arise from core ionization of the non-central carbon atom and consequently was assigned to a $1 \pi_g \longrightarrow 2 \pi_g$ transition. This assignment was made since these molecular orbitals exhibit nodes on the central carbon. This transition was also thought to be responsible for the most intense satellite in the O 1s spectrum.

Aarons et al., as in the case of CO_2 , applied the localized hole assumption and thereby calculated probabilities and energies of transitions. Table 2 shows the most intense O 1s and C 1s satellite as being assigned to a $3 \pi \longrightarrow 4 \pi$ transition ($2 \pi_u \longrightarrow 2 \pi_g$ in neutral molecule) and not to a $1 \pi_g \longrightarrow 2 \pi_g$ as proposed by Gelius et al. The assignments of Aarons et al.¹⁶ appear reasonable although their calculations do not agree absolutely with experimental data. However, the relative positions correlate and the O 1s satellites are correctly predicted to be more intense than the corresponding C 1s satellites. This is probably associated with the increased relaxation of the outer electrons after O 1s photoejection as opposed to C 1s ejection.

D. Organic Molecules

Shake-up satellites have been reported in some organic moieties.¹⁹⁻²² Pignataro et al. detected extra peaks in the C 1s electron spectra of thiophene, pyrrole and furan; (Figure 11) the satellite structure was absent in the analogous spectra of the corresponding alkyl derivatives. Gelius et al.²³ examined the heteroatom 1s electron spectra of these compounds and reported the absence of satellite structure (a result in accord with Pignataro's observations).

Aarons et al.¹⁶ attributed the absence of satellites in the heteroatom 1s spectra to the fact that since the symmetry (C_{2v}) is retained upon core ionization the only allowed transitions would be $a_2 \rightarrow a_2^*$, $b_1 \rightarrow b_1^*$ (π type) or $\sigma \rightarrow \sigma^*$. These transitions could not give rise to satellites close to the main peak (~ 10 eV) and hence were not observed. This same reasoning explains the lack of satellites in the C 1s spectrum of benzene if one considers a localized hole model ($D_{6h} \rightarrow C_{2v}$).

Pignataro et al.¹⁹ attributed the multi-peak structure in the C 1s spectra of the heterocyclic molecules to charge-transfer type transitions. The excitation is thought to consist of an electron in the π type molecular orbital with pronounced heteroatomic character jumping into an empty π^* M.O. Since experimental values of these π^* orbitals of the ion are not available, Pignataro et al. noted a correlation between observed ΔE (separation between satellite and main

peak) and the difference in ionization potential (Δ I.P.) between the first two peaks in the UV- photoelectron spectra of these compounds. The first band^{24,25} is assigned to an orbital of butadiene character and the second to the orbital largely of heteroatomic character. Both Δ E and Δ I.P. decrease in the order furan > pyrrole > thiophene. Photoelectron spectra of the five membered ring compounds indicates that heteroatom "lone pair p orbitals" do not exist as such, in accord with the aromatic nature of these substances.

According to Pignataro et al. electron shake-up of a charge-transfer type occurs with significant probability if core electrons are ejected from the acceptor atom(s). The positive hole is conducive for electron flow to the acceptor. A positive hole in the donor on the other hand is detrimental towards electron flow and the charge-transfer transition is less favored. Therefore, it is not surprising that satellite structure appears in the N 1s spectrum of nitrobenzene. It is known that nitrobenzenes in general show intramolecular charge-transfer transitions in absorption spectroscopy, in which an electron from the benzene ring is excited into an unoccupied π^* orbital of the nitro group.²⁶ Evidence that this type of a charge-transfer process is responsible for the satellite structure in the XPS spectrum comes from the consideration of o-dimethylnitroaniline. The N 1s XPS of this compound shows no satellite, a fact consistent with

the steric inhibition of resonance involving the ring π orbitals and the π^* orbital associated with the $-\text{NO}_2$ group.

E. Transition Metal Complexes

Shake-up satellites have been reported in the core and valence x-ray photoelectron spectra of a large number of first row transition metal complexes.²⁷⁻⁴⁵ These peaks typically appear less than 10 eV away from the main peaks and in some cases, e.g. CuF_2 ⁴⁰ and MnI_2 ,⁴⁶ are almost as intense as the main peaks. Several suggestions have been made concerning the exact nature of the valence excitation corresponding to the shake-up; it has been variously described as $3d \rightarrow 3d$, $3d \rightarrow 4s$, $3d \rightarrow 4p$ ^{27,35,40,43} or as a charge-transfer type transition.^{29,42,45} The balance of evidence however, seems to support the charge-transfer assignment as first proposed by Kim^{42,45} and Pignataro et al.²⁹

Kim based his argument on two observations:

(1) both the $3d \rightarrow 3d$ and $3d \rightarrow 4s, 4p$ transitions are forbidden by a rigorous application of the selection rules, except in cases where configuration interaction makes them allowed and (2) the transition energy for these two types of excitations do not agree with the transition energy as measured from XPS data. Pignataro et al. correlated satellite main peak splittings which he observed in the core electron spectra of $\text{Cr}(\text{CO})_6$, $\text{Cr}(\text{C}_6\text{H}_6)_2$ and $\text{Cr}(\text{C}_6\text{H}_6)(\text{CO})_3$ with known charge-transfer energies as measured from absorption spectro-

scopy. The transition energies measured by these two techniques are in close agreement (differing by $\sim .5$ eV or less). As in the case of the organic compounds, satellite peaks are expected in the core electron spectra of the acceptor species. Consequently a $M \rightarrow L$ charge-transfer shake-up will give rise to satellite structure in the ligand core electron spectra, while a $L \rightarrow M$ C-T transition will result in satellite(s) appearing in the metal core electron spectra. If a core electron is ejected, it is expected that the acceptor orbital will be stabilized and thus the transition energy will be decreased. This relaxation energy has been estimated to be 1-2 eV.⁴⁵ However some experimental evidence suggests that it is perhaps less than 1 eV for some transition metal complexes.⁴⁷

It is interesting to note that XPS data alone supports the charge-transfer mechanism as being responsible for the appearance of satellite peaks. For example, satellite structure has been observed in the 2p photoelectron spectra of some Sc(III) complexes.²⁸ A $3d \rightarrow 4s, 4p$ electron shake-up is therefore impossible because of the lack of 3d electrons. In addition, a $3d \rightarrow 4s$ transition could not account for the shake-up satellites seen in spectra of Mn(II) complexes. High spin Mn(II) is described by a 6A_1 ground state. Since the $3d^4 4s$ configuration cannot give rise to this state such an excitation is forbidden by the monopole selection rules. However, a shake-up satellite in Mn(II)

complexes has been observed. (Figure 12)⁴⁶ The $3d \rightarrow 4p$ transition is parity forbidden.

According to Kim, charge-transfer transitions involve only those orbitals having the same symmetry.⁴⁵ For example, in octahedral compounds transitions of a $L \uparrow t_{2g} \rightarrow Mdt_{2g}$ and $L 6 e_g \rightarrow Mde_g$ nature are allowed while in tetrahedral molecules $L \uparrow e \rightarrow Mde$ and $L t_2 \rightarrow Mt_2$ excitations can occur. Therefore one would expect to see different satellite structures in geometrically inequivalent complexes in which the metal and ligands involved are the same. We have in fact observed such differences. For example, the satellite-main peak intensity ratios for $CuCl_2$ and $CuCl_4^{2-}$ are .55⁴⁰ and .22⁴⁸ respectively. In addition, the satellite-main peak splittings differ as well. In fact, it has been noted that the intensities and positions of peaks can be explained or even predicted by taking into account the C-T transitions that are energetically plausible and their relative probabilities as determined by the sudden approximation.⁴⁷ For example, the Fe 2p spectrum of $K_3Fe(CN)_6$ exhibits a low intensity satellite probably of a $L \uparrow t_{2g} \rightarrow Mdt_{2g}$ nature while the analogous spectrum of $K_4Fe(CN)_6$ appears to be devoid of satellite structure. The latter complex has a $t_{2g}^6 e_g^0$ configuration as a consequence of a large crystal field splitting thereby making a $L 6 e_g \rightarrow Mde_g$ transition of large energy and therefore improbable. For the same reason low spin Co(III) complexes do not appear

to give rise to satellites in their metal core electron spectra.³⁷ It should be mentioned that in general, for the same type of transition, the probability and consequently the intensity of satellite peaks increases as the transition energy decreases. For example, as one proceeds from MnF_2 , to CoF_2 ³⁵ the $L\pi \rightarrow t_{2g}$ transition decreases in energy and therefore an increase in intensity is observed. This trend has also been noted for chloride complexes.

Charge-transfer type transitions are known to occur in the absorption spectra of an innumerable number of complexes. Consequently, comparisons between the two sets of data could be of significance as long as the transitions involved are of the same nature. As already mentioned Pignataro made such comparisons for a few Cr complexes. We have also compared the C-T transition energies of some tetrahedral first row transition metal halide complexes obtained from UV data with those values obtained from XPS spectra.⁴⁷ The excellent agreement implies the potential application of satellite-main peak splittings to the assignment of absorption bands in optical spectroscopy.

At this time only the core electron spectra of Cu and Ni⁴²⁻⁴⁵ in their complexes have been reported to any significant degree. Consequently, the satellite structure has been examined more closely for those two metals than for any of the other transition metal complexes. Frost et al.⁴⁰ studied 46 Cu(II) and Cu(I) complexes and noted satellites

only in the spectra of the divalent copper complexes (Figure 13). Since Cu(I) is known to have a $t_{2g}^6 e_g^4$ configuration C-T transitions of a ligand to metal d orbital nature are impossible. Any other allowed transition would be of very large energy and thus improbable. The only probable transition for Cu(II) complexes would be of a $L 6 e_g \rightarrow Mde_g$ nature. One therefore would expect only one satellite peak for example in the Cu(II) 2p core electron spectra. Two satellite peaks for a number of Cu compounds, however, have been reported which perhaps can be attributed to the tetragonal distortion (Jahn-Teller effect) which is known to occur in octahedral type Cu(II) complexes.⁴⁵ Such a distortion would reduce the symmetry of the molecule and thus split the d orbitals even further making additional transitions possible. It is interesting that some Ni(II) complexes also show two satellite peaks accompanying each Ni 2p main peak. The excited Ni(II) molecule (the molecule after the $L 6 e_g \rightarrow Mde_g$ transition has occurred) should also be subject to a Jahn-Teller distortion as well. It appears that a study which correlates satellite structure with known tetragonally distorted molecules would be useful at this time. In this context, we have noted the appearance of more than one satellite in the core electron spectra of some metal acetylacetonates in which the symmetry is reduced from octahedral to trigonal. Such reduction again results in a further splitting of d orbitals and makes possible

several allowed transitions. In fact experimental evidence suggests that information concerning structure of metal complexes can be derived from examination of satellite structure. Matienzo et al.⁴⁴ for example noted the absence of satellites in the Ni(II) 2p spectra of square planar complexes.

It seems evident at this point that shake-up satellites in the core electron spectra of transition metal complexes result from a charge-transfer type transition. It appears that if $M \rightarrow L$ or $L \rightarrow M$ charge transfers are observed in absorption spectra then such transfers will appear in XPS as long as they are allowed by the selection rules. In addition, it seems reasonable to expect satellites ($L \rightarrow M$) in core electron spectra of transition metals in complexes having π bond character and to expect satellites in core electron spectra of ligands ($M \rightarrow L$) having low lying π^* type empty orbitals e.g. CO, CN, aromatics. For example, satellites have been reported in the O 1s and C 1s spectra of some metal carbonyls and in the O 1s spectra of some metal acetates.⁴⁷ It should be noted that satellite positions and intensities are functions of both the nature of the metal and ligands, and the symmetry of the complex.

F. Rare Earth Compounds

Charge-transfer shake-up satellites have been observed by Jorgensen and Berthou⁴ and Wertheim et al.⁵ in the metal

3 d electron spectra of some rare earth compounds. The latter workers reported satellites in the trifluoride complexes of the rare earths from La to Sm. These extra bands are thought to arise from negative charge being transferred from the valence band (ligand character) to the empty metal 4f levels upon 3 d electron emission. Consequently, one would expect a decrease in satellite-main peak separation and an increase in intensity upon changing the metal from La to Nd. Such a trend is experimentally observed. Resolved satellite structure is not observed beyond Sm, since the 4f level approaches the valence band level. In addition, there is a decrease in overlap between the 4f and valence band orbitals.⁴

Jorgensen and Berthou observed satellites in the 3 d electron spectrum of seven La(III) compounds.⁵ A charge-transfer mechanism again is thought to give rise to the extra peaks. It was pointed out that there should be a similarity between the one electron wavefunctions of Ce(IV) and La(III) with a positive core hole. Ce(IV) is known to give rise to intense charge-transfer bands in absorption spectra. These bands indicate that the unoccupied 4f orbitals of the ground state must overlap well with the filled ligand orbitals. Therefore, the appearance of satellite peaks in the La(III) 3 d photoelectron spectra adds further evidence to support the charge-transfer assignment. It should also be noted that as expected the LaF₃ spectrum showed the largest

E and smallest satellite intensity. The satellites were approximately as intense as the main peaks in those La(III) complexes where oxygen is bound to the metal (see Figure 14).

Satellites have also been seen in the 4f electron ESCA spectra of some U(VI) compounds.^{5,6} Jorgensen and Berthou⁵ reported them in the U 4f electron spectrum of $\text{Rb UO}_2 (\text{NO}_3)_3$ with a satellite to main peak intensity ratio of approximately 1:5. In light of all the work already described in this review, it seems reasonable to attribute these satellites to a ligand electron being transferred to the U 5f shell. We have also noted extra peaks in the U 4f spectra of some uranyl pyridine carboxylic acid complexes (Figure 15). The intensities are low ($\sim 10\%$) and the satellite-main peak separation are of the order of 2 -4 eV.

Jorgensen suggested that the low energy (~ 3 eV) bands in the absorption spectra of many uranyl complexes are due to a charge-transfer of an electron from a ligand orbital to an empty 5f orbital in the central U atom.⁴⁹ However, many other workers assign the transition to a charge-transfer within the UO_2^{+2} c species.^{50,51} McGlynn and Smith⁵¹ stressed the significance of π bonding in the UO_2^{++} grouping and thus assigned these low energy absorption bands to an excitation of an electron from the highest filled π^* orbital to a non-bonding orbital on uranium. Calculations show only limited participation of 5f orbitals in bonding. Since all of the compounds we examined contained the UO_2^{++} cation,

the transition described by McGlynn and Smith may be responsible for satellite structure. However it should be noted that in some of our spectra more than one satellite appeared 2 -4 eV from the main peak (Figure 8). It is possible that in these cases ligand electrons are being transferred to the U 5f orbital as well, as suggested by Jorgensen. The low intensity of these satellite bands can be attributed to the small overlap between the donor and acceptor orbitals.

III. CONCLUSION

The sudden approximation coupled with other arguments in many cases has been able to describe the exact electronic transition giving rise to the shake-up satellite peaks observed in the electron spectra of the various systems investigated. Either quantitative or qualitative evidence has been presented in each case to support the assignments made. It is apparent that satellite positions and intensities convey a wealth of information concerning, for example, the nature of the ligands, bonding, electronic configuration and geometry of transition metal complexes. Further studies are needed which focus on the effect of each of these variables on the satellite peaks in the core electron spectra of transition metals. In addition, satellite structure has not been examined in the spectra of second and third transition metal complexes although absorption spectra of many of these

compounds e.g. halides are rich in charge-transfer bands.

It should be noted that we have concentrated on core electron spectra and have not described shake-up satellites in valence band spectra to any significant degree. Hammett and Orchard⁵² have reviewed most of this work. In addition, satellite peaks have been reported in vuv photoelectron spectroscopy by Cradock and Duncan⁵³ in their work on CSe₂. It should also be mentioned that since the primary purpose of this review is to acquaint the chemist with the various types of molecules that show this extra structure in core electron spectra, and to describe the type of information that can be derived from shake-up peaks, the references we have given are not all inclusive.

Table 2.1

Calculated and Experimental Satellite States
In the Ne1s Photoelectron Spectrum

Shake-up		Calc. Excitation Energy ΔE (eV)	Exp. Ne1s Spectrum (eV)	Na ⁺ Optical Spectrum (eV)
2p \rightarrow 3p	² S	35.59	37.3	36.36
2p \rightarrow 3p	² S	39.46	40.7	38.29
2p \rightarrow 4p	² S	40.50	42.3	
2p \rightarrow 5p	² S	42.38	44.2	
2p \rightarrow 4p	² S	44.62	46.4	
2s \rightarrow 3s	² S	61	60	

Table 2.2

Shake-up Probabilities For CO, CO₂ and C₃O₂

	Hole State	Assign-ment	Intensity (%) (relative to the total peak intensity)		ΔE (eV)	
			Calc.	Exp.	Calc.	Exp.
CO	C 1s	2 σ \rightarrow 4 σ	2.9		24.0	
		3 σ \rightarrow 4 σ	.7	~ 3	18.1	10-30
		1 π \rightarrow 2 π	.4		16.7	
	O 1s	2 σ \rightarrow 4 σ	0.0		24.1	
		3 σ \rightarrow 4 σ	1.0	~ 6	16.4	10-30
		1 π \rightarrow 2 π	6.1		18.0	
CO ₂	C 1s	2 σ_u \rightarrow 3 σ_u	4.0	~ 6	24.2	18
		1 π_u \rightarrow 2 π_u	0.5	-	18.3	-
	O 1s	3 σ \rightarrow 5 σ	0.0	-	19.0	-
		2 π \rightarrow 3 π	9.0	~ 8	15.0	16
C ₃ O ₂	C 1s (central)	3 σ_g \rightarrow 4 σ_g	.8	-	18.0	-
		2 π_u \rightarrow 3 π_u	5.9	~ 20	14.5	14
	C 1s (non-central)	2 π \rightarrow 4 π	0.5	-	16.1	-
		3 π \rightarrow 4 π	5.0	~ 15	9.3	7.9
		3 π \rightarrow 5 π	0.3	-	21.8	-
	O 1s	2 π \rightarrow 4 π	0.9	~ 15	17.5	16
		3 π \rightarrow 5 π	0.7		16.3	
		3 π \rightarrow 4 π	16.1	~ 20	10.9	8.2

Part 2. Satellite Peaks in the X-Ray Photoelectron Spectra of Mn(II) Complexes

The origin of satellite peaks in transition metal complexes has been variously attributed to shake-up transitions of a metal $3d \longrightarrow 4s$ nature^{27,35} or of a ligand orbital to metal orbital charge-transfer type.^{41,42} Although the latter explanation has been favored in recent publications,²⁸ it is desirable that a body of confirmatory evidence be obtained to support it. In addition, it is desirable that measurements of the energies and intensities of the satellite peaks be taken on meaningful series of compounds.

Mn(II) compounds represent a useful series for investigating satellite peaks associated with the metal 2p main peaks, especially if the compounds contain anionic species of approximately known electronegativities. Thus, we have examined the Mn 2p photoelectron spectra of MnS, MnTe, MnCl₂, and MnI₂. Satellite structure is observed in every case (see Figure 12).

High spin Mn(II) octahedral complexes are characterized by a 6A_1 ground state configuration. A $3d \longrightarrow 4s$ transition would result in a $3d^44s$ configuration, for which the only possible sextet states are 6E and 6T_2 .² The appropriate selection rules governing the shake-up transition are derived from the Sudden Approximation theory: when the theory is applied to shake-up in transition metal compounds, the minimum rules are $\Delta L_V = \Delta S_V = 0$ where L_V is the total valence orbital

angular momentum and S_V is the total spin angular momentum. Thus, it is apparent for Mn(II) compounds that a $3d \rightarrow 4s$ shake-up transition is forbidden since formation of either a 6E or 6T_2 state would violate the $\Delta L_V = 0$ selection rule. Thus, the satellite structure must be attributed to a shake-up of charge transfer type. Indeed it is possible to account for trends in the intensities and peak positions of the satellites based upon this assumption.

The following major trends were noticed:

As the ligand-to-metal bond becomes more covalent,

- (a) the intensity of the satellite structure compared to the intensity of the main peak increases
- (b) the separation in energy between the satellite and main peak decreases

A consideration of charge transfer theory reveals that these trends are consistent with the type of transitions possible. The only transitions that might be expected to occur with any significant probability are of a ligand $\uparrow t_{2g} \rightarrow$ metal dt_{2g}^a type, and of a ligand $e_{eg} \rightarrow$ metal de_g^a type (a = antibonding).⁴¹ The latter can be discounted because of the large energy difference between the orbitals;⁵⁴ this would result in a correspondingly large satellite to main peak spacing, certainly much larger than that observed. Thus, the nature of the charge transfer transition responsible

for the satellite structure is $L \pi t_{2g} \longrightarrow Mdt_{2g}^a$
 (L = ligand, M = metal).

Considering now the Mn(II) halides, the energy of the $L \pi t_{2g}$ orbital will increase as the ligand is changed from F through group VII to I. This will result in a progressively smaller energy difference between the $L \pi t_{2g}$ and Mdt_{2g} orbitals, which is reflected in the smaller satellite-to-main peak spacings observed. The transition probability will also increase as the group is descended, owing to increased orbital overlap, and this is mirrored in the increasing satellite peak intensity. Similar, but less dramatic effects are seen in the Group VI Mn(II) photoelectron spectra.

Since it appears, then, that satellite intensities and peak positions are functions of covalency, correlations should exist between multiplet-splittings and satellite splittings and intensities. According to Carver et al.,⁵⁵ the 3s multiplet splittings of MnF_2 , $MnCl_2$, and $MnBr_2$ are respectively 6.3 eV, 6.0 eV, and 4.8 eV--thus being in the same relative order as our satellite splittings and intensities.

Part 3. Correlations Between (a) Geometry of the Complex and Satellite Structure, and (b) Between Satellite Splittings and Energies of UV Charge-Transfer Bands

Pignataro et al. have observed satellite peaks in the core electron spectra of some chromium complexes which he attributed to the charge-transfer process.²⁹ In addition,

correlations were noted between the charge-transfer excitation energies as measured from satellite-to-main peak splittings and the corresponding energies as obtained from UV absorption spectroscopy. Good quantitative agreement was found between the two sets of data. This prompted us to investigate the possible application of satellite peak positions to the problem of peak assignments in absorption spectroscopy. It is well known that the optical spectra of many important biochemical substances are so plagued with absorption bands that assignment of peaks to particular transitions is an arduous, if not impossible task.

Consequently, we now report some preliminary results which (a) support the charge-transfer explanation of satellite peaks proposed by Pignataro and Kim, in addition suggest a relationship between the geometry of the molecule and the intensity of satellite peaks, and (b) imply that satellite data is of potential use as an aid in the interpretation of absorption spectra.

The metal 2p photoelectron spectra of several first row transition metals were examined in both their octahedral and tetrahedral complexes. In several cases correlations were made between optical absorption data and the corresponding ESCA data for these complexes as well as for some metal acetylacetonate complexes.

EXPERIMENTAL

Because of the volatility of the metal acetylacetonates, samples were run on the cryogenic probe (-10°C) of the Hewlett-Packard 5950 ESCA model. The Flood gun was employed in order to reduce charging effects. A spectrum was recorded after counting for approximately 20 minutes. It was noted that the O 1s peaks and corresponding satellite structures did not undergo change in relative intensity or position with time which negates the possibility of H_2O contributing to the bands.

The ESCA spectra of $\text{Ni}(\text{acac})_2$ ⁴³ and parts of $\text{Cr}(\text{acac})_3$ ⁵⁶ (acac=acetylacetonate) have been reported elsewhere, however O 1s satellites were not mentioned in either of these works. The satellite-to-main peak intensity ratios reported in Tabel 3 were determined by planimetry.

Results and Discussion

As indicated by Table 2.3, the satellite intensities of the Mn(II), Co(II) and Cu(II) octahedral chlorides differ noticeably from their tetrahedral analogs. It is apparent that for the Mn(II) chlorides the satellites are more intense for the tetrahedral geometry, while for Co(II) and Cu(II) compounds the reverse is true--the satellites are more intense in the octahedral complexes. For appropriate pairs

of Fe(II) and Ni(II) compounds, the satellite intensity seemed essentially the same for both tetrahedral and octahedral geometries.

The intensity differences noted are explicable in terms of allowed charge-transfer transitions. For octahedral symmetry, two transitions are allowed: $L \pi t_{2g} \longrightarrow Mdt_{2g}$ and $L \sigma e_g \longrightarrow Mde_g$ (L = ligand, M = metal). In tetrahedral symmetry, three charge-transfer transitions are allowed which could give rise to the observed satellites: $Lt_2(2) \longrightarrow Mdt_2(3)$, $Lt_2(1) \longrightarrow Mt_2(3)$, and $L \sigma e(1) \longrightarrow Mde(2)$.

The satellite intensities (i.e. ratio of area of satellite peak to area of main peak, viz. for metal $2p_{3/2}$) can be accounted for in the light of these differing numbers of allowed transitions, and the relative probabilities of each transition. These relative probabilities are determined approximately from the overlap integrals of the wave-functions pertaining to the ligand and metal type molecular orbitals involved in the charge-transfer.⁴ This in turn is related to the energy difference (ΔE) between the energies of the donor and acceptor orbitals.

First of all, considering Mn(II) compounds, the spectra reveal more intense satellites accompanying the Mn 2p main peaks in the tetrahedral rather than in the octahedral complex. In octahedral symmetry, only one transition, $L \pi t_{2g} \longrightarrow Mt_{2g}$, is reasonable. The $L \sigma e_g \longrightarrow Mde_g$ transition will not contribute significantly to satellite

peak intensity owing to the large ΔE .⁵⁴ In tetrahedral symmetry, however, two transitions are energetically reasonable: $L \sigma e \longrightarrow Mde$, and $Lt_2(2) \longrightarrow Mdt_2(3)$. Thus, it is logical to attribute the increased intensity for the tetrahedral Mn(II) species to the increased number of charge-transfer transitions.

The larger intensity of the satellites in the Co 2p photoelectron spectrum of $CoCl_2$ as compared with the corresponding satellites in the $CoCl_4^{2-}$ spectrum can also be explained by considering the most probable transitions. For the tetrahedral complex the $L \sigma e \longrightarrow Mde$ transition cannot occur since the metal de orbitals are already filled. Furthermore, only the $Lt_2(2) \longrightarrow Mdt_2(3)$ transition is in accord with the observed ΔE (see Table 2). Also in the octahedral case only one transition, $L \pi t_{2g} \longrightarrow Mt_{2g}$ ⁵⁷ is probable. Therefore, according to the Sudden Approximation, the overlap integral involving donor and acceptor wavefunctions must be larger in the octahedral case. This is reasonable since in general ligand π orbitals can interact with all metal d orbitals (e and t_2) in tetrahedral molecules, while in octahedral symmetry the ligand π type orbitals interact only with the metal dt_{2g} orbitals. Consequently, the $t_2 \longrightarrow t_2$ type transition would have a smaller probability as compared to the $t_{2g} \longrightarrow t_{2g}$ transition.

The spectra of $CuCl_2$ and $NiCl_2$ both show intense satellite structure. The only charge-transfer type excitation

possible would be one of a $L \sigma e_g \longrightarrow Mde_g$ nature. This is expected to occur with high probability owing to the correspondingly large de_g/e_g interaction.⁵⁸ In general Cu(II) and Ni(II) octahedral complexes show very intense satellite peaks in their core electron spectra.^{40,44} For tetrahedral $CuCl_4^{2-}$, which shows weaker satellites, two transitions are possible, $Lt_2(2) \longrightarrow Mt_2(3)$, and $Lt_2(1) \longrightarrow Mt_2(3)$, but the latter is discounted because of the large energy difference between the orbitals.

Other trends are of interest. A comparison of the spectra of the metal 2p x-ray photoelectron spectra of the series MnF_2 , FeF_2 , and CoF_2 reveals that the satellites become more intense and the separation of satellite peak to main peak becomes smaller as the series is ascended.³⁵ This observed trend is consistent with the assignment of a $L \pi t_{2g} \longrightarrow Mdt_{2g}$ transition as being mainly responsible for the satellite peak. On going from Mn(II) to Co(II), the dt_{2g} orbitals are being stabilized, thus decreasing ΔE , and producing the observed effects on the spectra. This series is interrupted by NiF_2 and CuF_2 both of which show a smaller satellite-main peak splitting than that which is observed in the CoF_2 spectrum. This is to be expected since in the latter two complexes the satellites result from a $L \sigma e_g \longrightarrow Mde_g$ transition.

A further trend is apparent from the spectra appearing in the work of Escard et al.⁴⁸ on tetrahedral transition

metal complexes. For the series in which the complex anion is kept constant and the alkyl group R, on the cation, $(R_4N)^+$ is changed to a more electron donating species, the metal 2p satellite intensities decrease, a trend consistent with the expected destabilization of the metal acceptor orbital and consequent decrease in probability.

Tables 2.4 and 2.5 indicate some charge-transfer energies obtained from UV and ESCA spectra. The good correlation is surprising since upon electron photoejection the metal acceptor orbital is stabilized. Therefore, the transition energy as taken from ESCA data should be less than the corresponding energy acquired from absorption data. In fact it has been estimated that the two should differ by 1-2 eV,⁴⁵ the shake-up transition being of lower energy. The almost exact correlation perhaps results from the electron shake-up occurring simultaneously with photoejection so that the energy of the valence orbitals involved do not change appreciably from the ground state energies.

The metal acetylacetonates were investigated by the authors since they are known to display both $L \longrightarrow M$ and $M \longrightarrow L$ charge-transfer bands in their absorption spectra. It is known for example, that $Fe(acac)_3$ ^{59,60} exhibits both types of C-T transitions, while $Cr(acac)_3$ ^{60,61} gives rise to only a $M \longrightarrow L$ transition and $Ni(acac)_2$ ⁶² displays only a $L \longrightarrow M$ type. It might therefore be predicted a priori that satellite structure would be observed to the higher

binding energy side of the metal 2p peaks of $\text{Fe}(\text{acac})_3$ and $\text{Ni}(\text{acac})_2$ (but not in that of $\text{Cr}(\text{acac})_3$) while 0 1s satellites would appear for $\text{Fe}(\text{acac})_3$ and $\text{Cr}(\text{acac})_3$. Table 3 shows the good agreement between the predicted and actual results. The broadness of the peaks and low intensity of the satellites preclude a precise measurement of the C-T transition energy.

The molecular symmetry of the acetylacetonates investigated is reduced from octahedral to trigonal (D_3) in both $\text{Fe}(\text{acac})_3$ and $\text{Cr}(\text{acac})_3$ while the point group of $\text{Ni}(\text{acac})_2$ is uncertain owing to its tendency to form a trimer in the solid state.⁶³ As a result of the lowering of symmetry the t_{2g} orbitals split into an a_1 and e pair of levels. The Sudden Approximation requires donor and acceptor orbitals to have the same symmetry; thus trigonal symmetry increases the number of allowed transitions all of which are expected to have widely differing energies. Recent calculations⁶⁰ have indicated the allowed transitions and their approximate energies. It appears that the transitions noted from core electron ESCA spectra constitute only a fraction of those allowed by the Sudden Approximation. The expected effect of these other transitions is to steal intensity from those satellite bands clearly observed. If a transition took place at higher energy than the observed satellite, it might escape detection since a higher energy transition would not be as favorable a process as a corresponding lower energy

transition. On the other hand, if the transition took place at a lower energy than the observed satellite, it will contribute to peak broadening and thus be unobservable. The clear asymmetry of the metal 2p peaks in the $\text{Fe}(\text{acac})_3$ and $\text{Ni}(\text{acac})_2$ spectra lends support to this observation. It should be pointed out that the intensity of the satellite peaks observed in the metal core electron spectra could not be calculated because of the large asymmetric main peak which overlapped with the satellite band. In addition, it should also be mentioned that the O 1s peaks were slightly asymmetric. This may result from some unpaired electron spin density from the metal being transferred to the ligands via delocalized molecular orbitals.

The results of the metal acetylacetonate investigation indicate the importance of stereochemistry on the position and intensity of satellite peaks. Therefore, it should be noted that the transitions assigned to the satellite structure in the metal halides apply only to strictly octahedral or tetrahedral molecules. For example, it is known that octahedral type Cu(II) complexes undergo tetragonal distortions which reduce the molecular symmetry and thus split the metal d orbitals even further. This distortion may very well be responsible for the appearance of two satellite peaks in the core electron spectra of some Cu(II) complexes.⁴⁰ In fact a distorted excited state may be responsible for the appearance of two peaks in the

corresponding spectra of some Ni(II) complexes.⁴⁴ Such distortions are a result of the Jahn-Teller effect; however it is possible that spin-orbit splitting can give rise to additional allowed transitions which may result in the appearance of more satellite peaks than anticipated.

Table 2.3

Satellite Intensities in the Tetrahedral
and Octahedral Chloride Complexes

	Satellite to Main Peak Intensity Ratio ($2p_{3/2}$)
MnCl ₂	.18 ^a
MnCl ₄ ²⁻	.38 ^b
FeCl ₂	.5 ^a
FeCl ₄ ²⁻	.5 ^e
CoCl ₂	1.0 ^f
CoCl ₄ ²⁻	.48 ^b
NiCl ₂	.6 ^c
NiCl ₄ ²⁻	.59 ^b
CuCl ₂	.55 ^d
CuCl ₄	.22 ^b

a Spectra were obtained by the authors on a Hewlett-Packard Photoelectron Spectrometer.

b Values taken from ref. 48. The cation in each case was (Et₄N)⁺.

c Value obtained from the spectrum shown in ref. 44.

d Value give in ref. 40.

e Value obtained from the spectrum shown in ref. 31.

f Value obtained from the spectrum shown in ref. 36.

Table 2.4

Comparison of UV and ESCA Data for the
 $Lt_2(2) \longrightarrow Mt_2(3)$ Transition

	UV Absorption Energy (eV)	Satellite to Main Peak Separation (ΔE) ($2p_{3/2}$) (eV)
$FeCl_4^{2-}$	4.9 ^a	5.0 ^b
$CoBr_4^{2-}$	4.6 ^c	4.5 ^b
$CoCl_4^{2-}$	5.2 ^a	5.0 ^b
$NiCl_4^{2-}$	5.3 ^c	5.6 ^b

a ΔE measured from spectrum shown in ref. 65.

b ΔE measured from spectrum shown in ref. 48.

c ΔE measured from spectrum shown in ref. 64.

Table 2.5

Comparison of the Optical Charge Transfer
Energies and the Separation of the
Satellite and Main Photoelectron
Peaks

	<u>Fe(acac)₃</u>	<u>Cr(acac)₃</u>	<u>Ni(acac)₂</u>
a) Optical Charge Transfer Energies (eV)			
L → M	2.9	-	5.5
M → L	3.5	4.0	-
b) Separation of Main and Satellite Peaks (eV)*			
metal 2p _{3/2}	2.8 (4.6) ^a	- (3.2) ^a	5.3 (8.4) ^a
metal 2p _{1/2}	3.2	-	5.8
oxygen 1s	4.1 (2.1) ^a	4.3 (2.4) ^a (.09) ^b	- (2.0) ^a

*The peak separations are estimated to be accurate to within 0.5 eV.

a FWHM values (Rising base line made 2p_{1/2} halfwidths difficult)

b Satellite-main peak intensity ratios

Fig 8

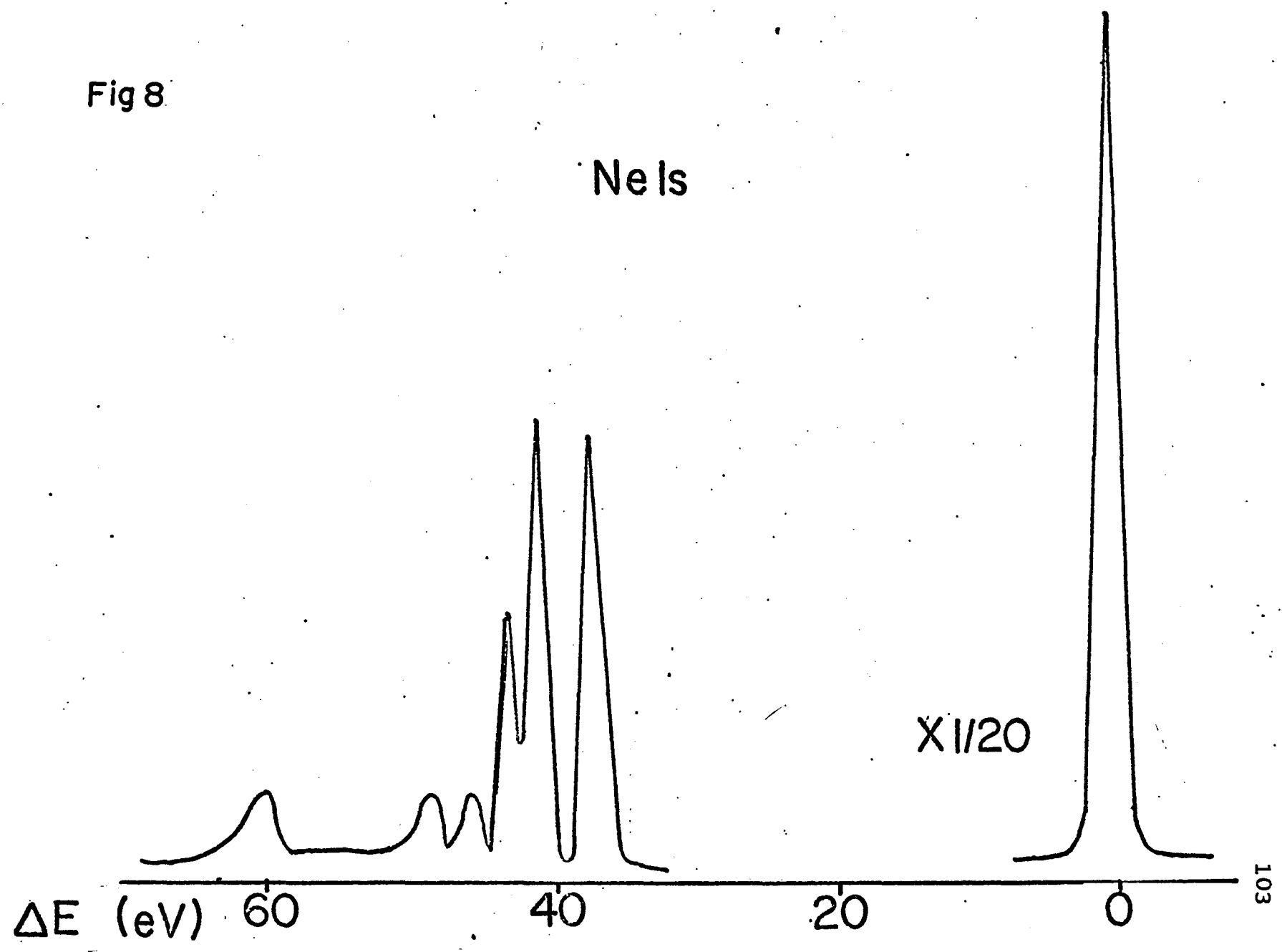
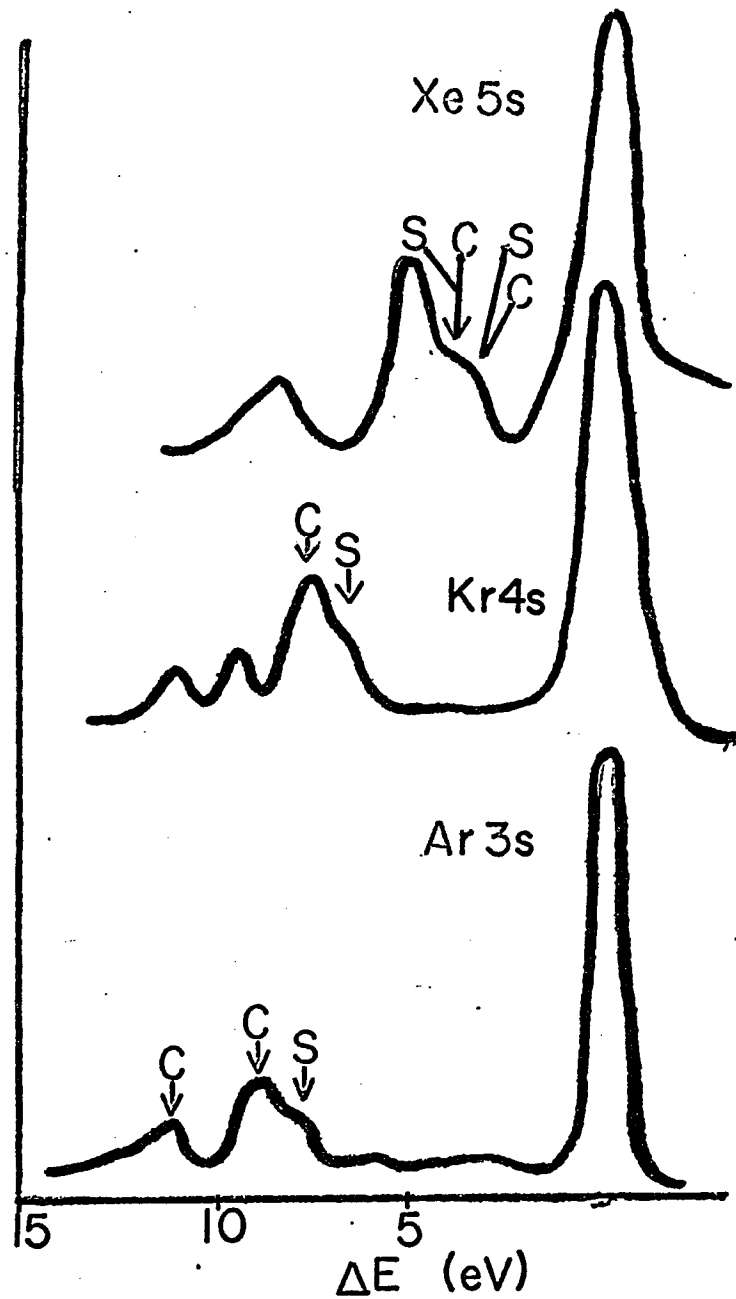
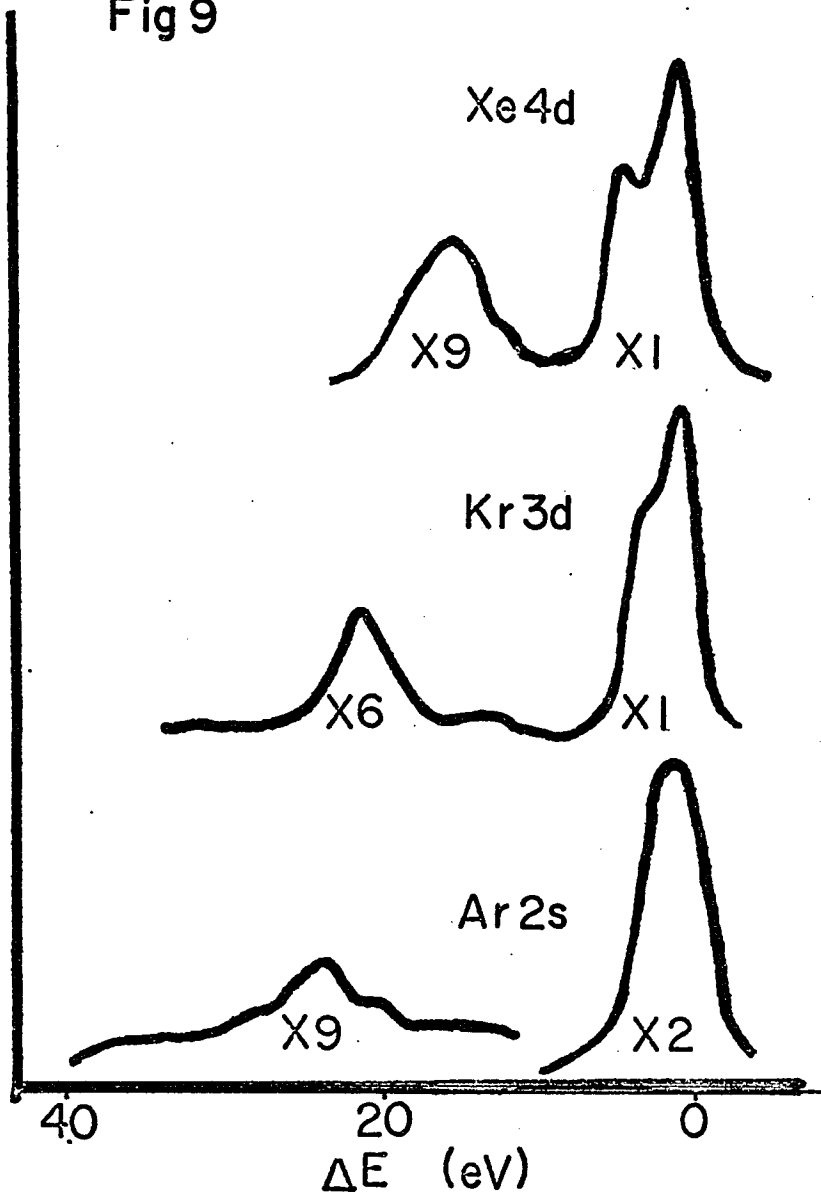


Fig 9



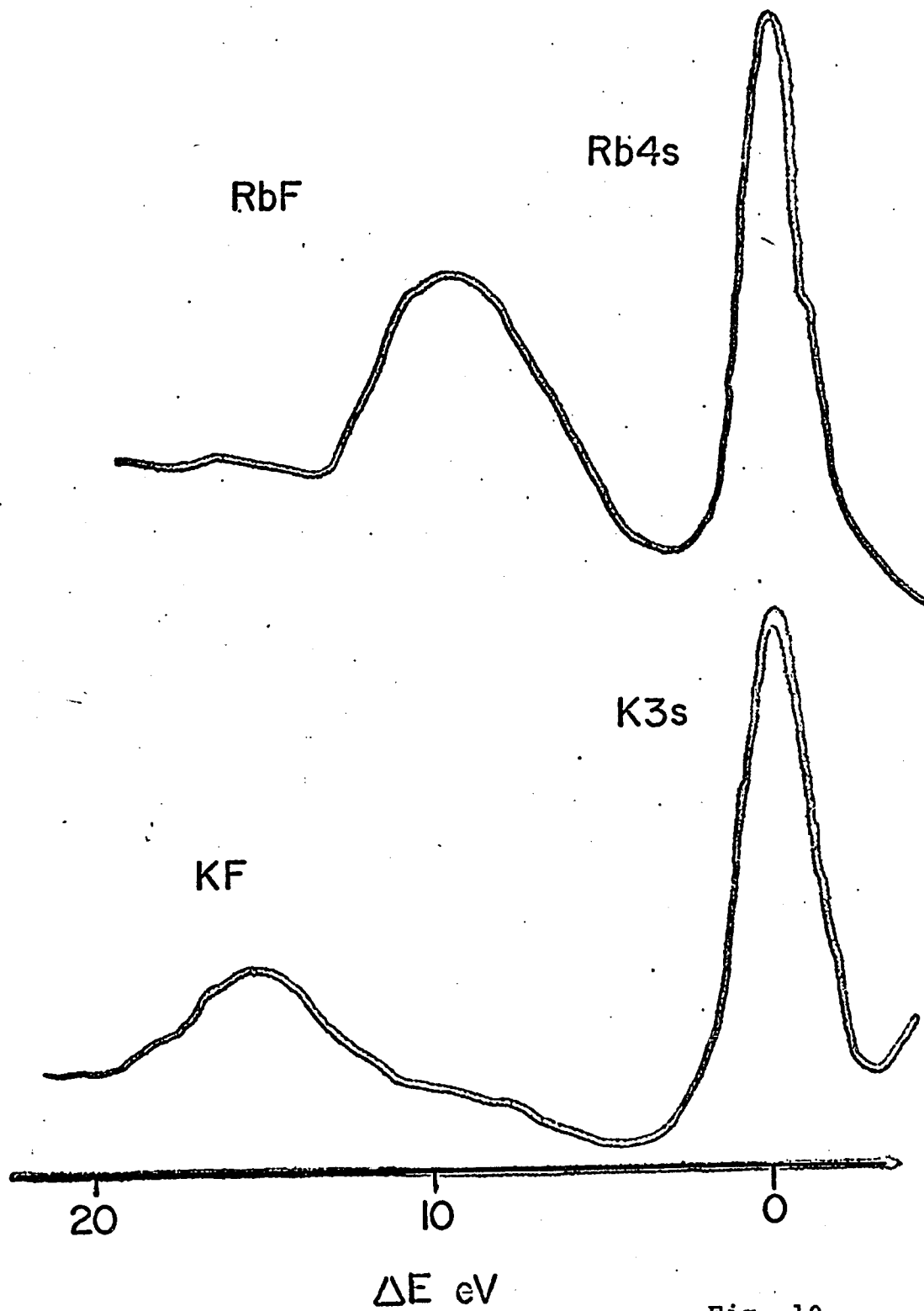


Fig. 10

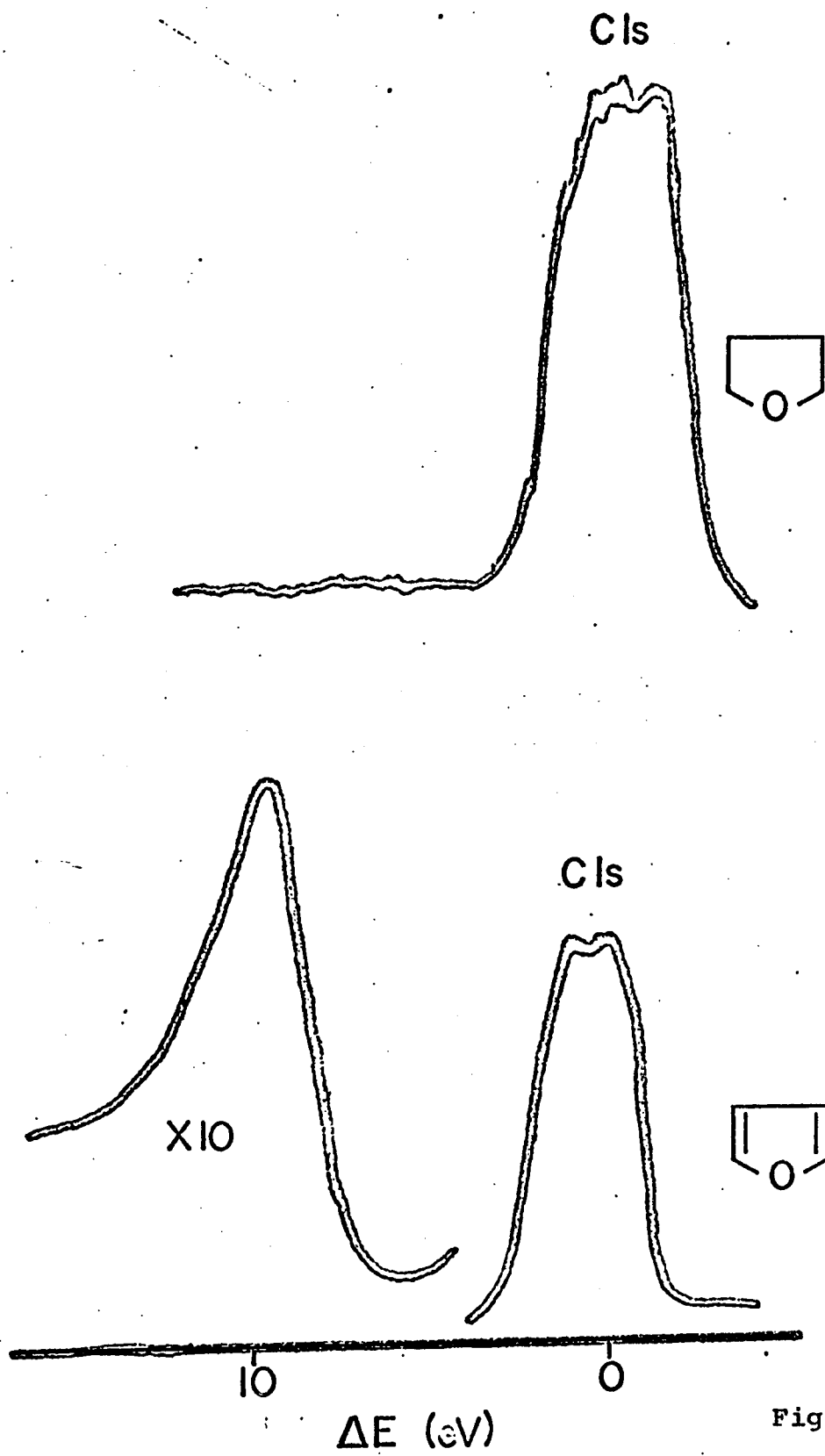


Fig. 11

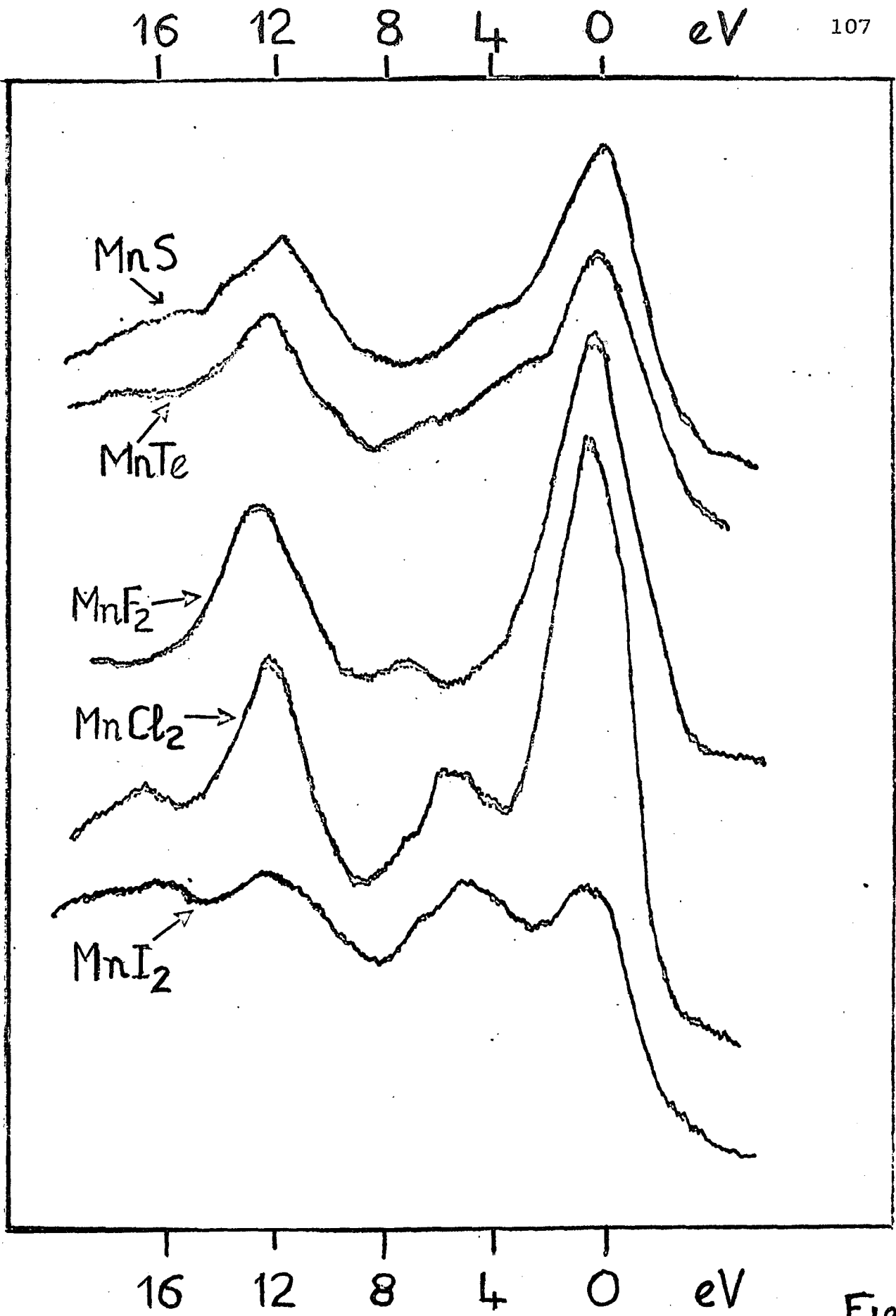


Fig 12

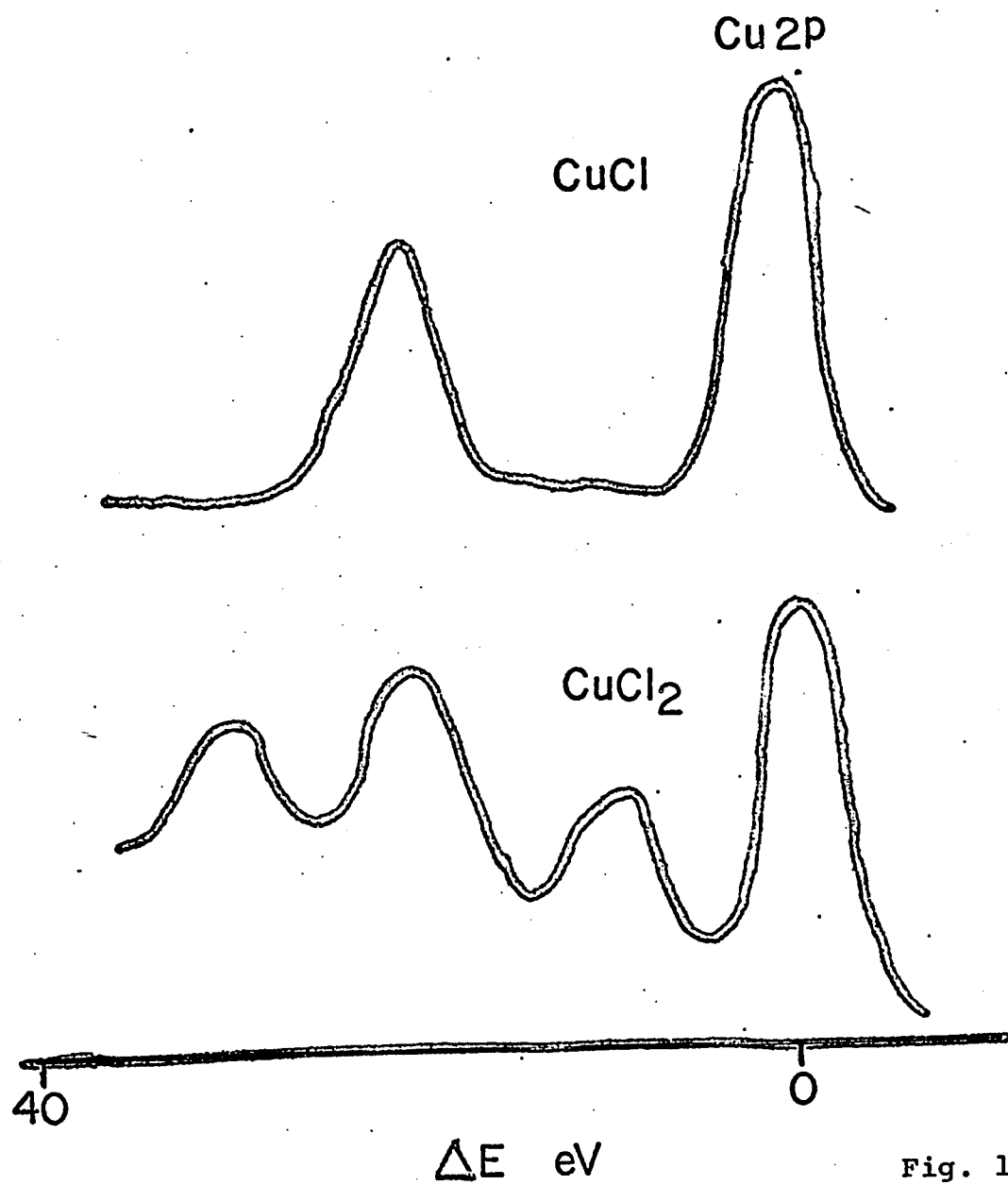


Fig. 13

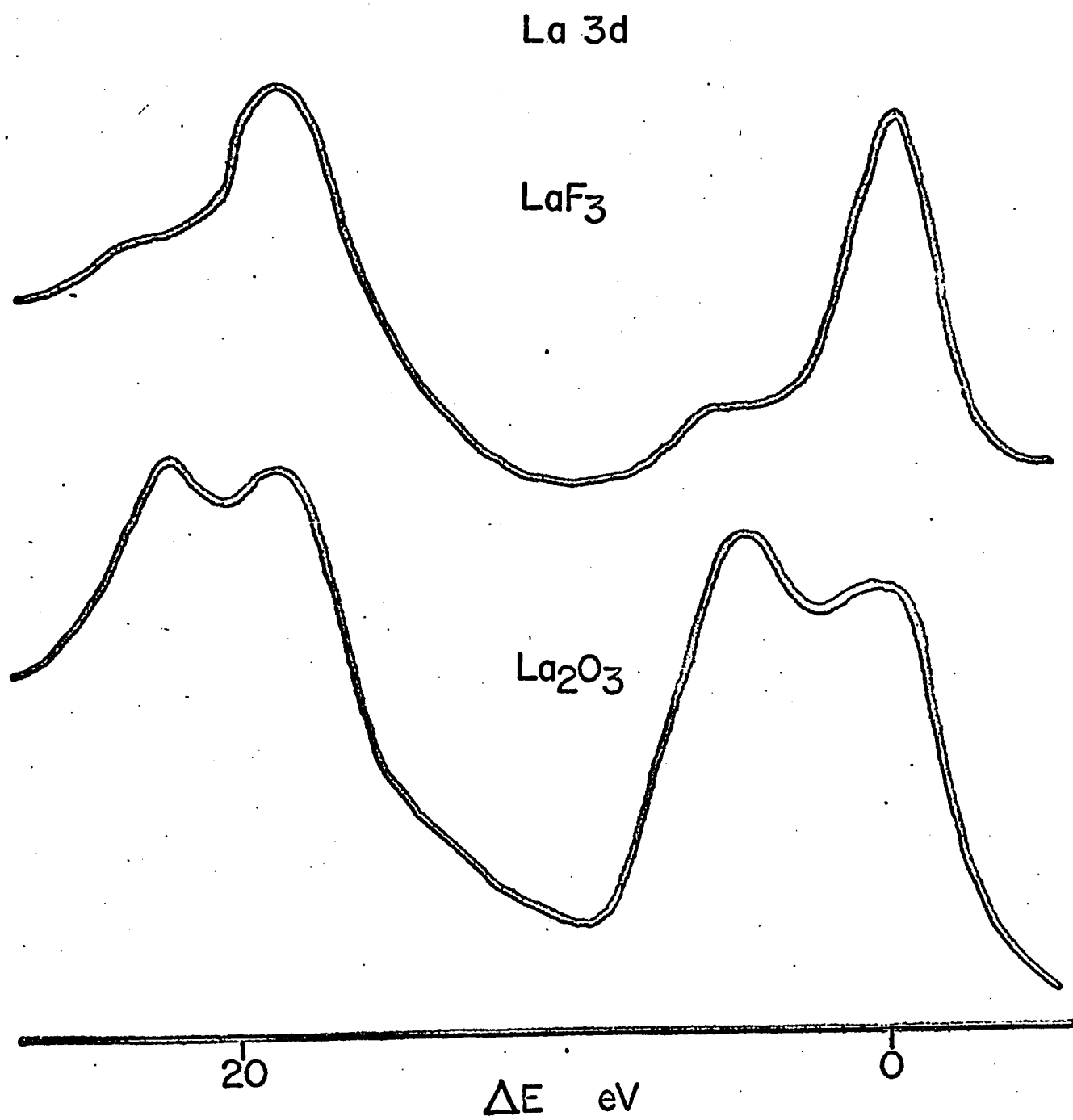


Fig 14

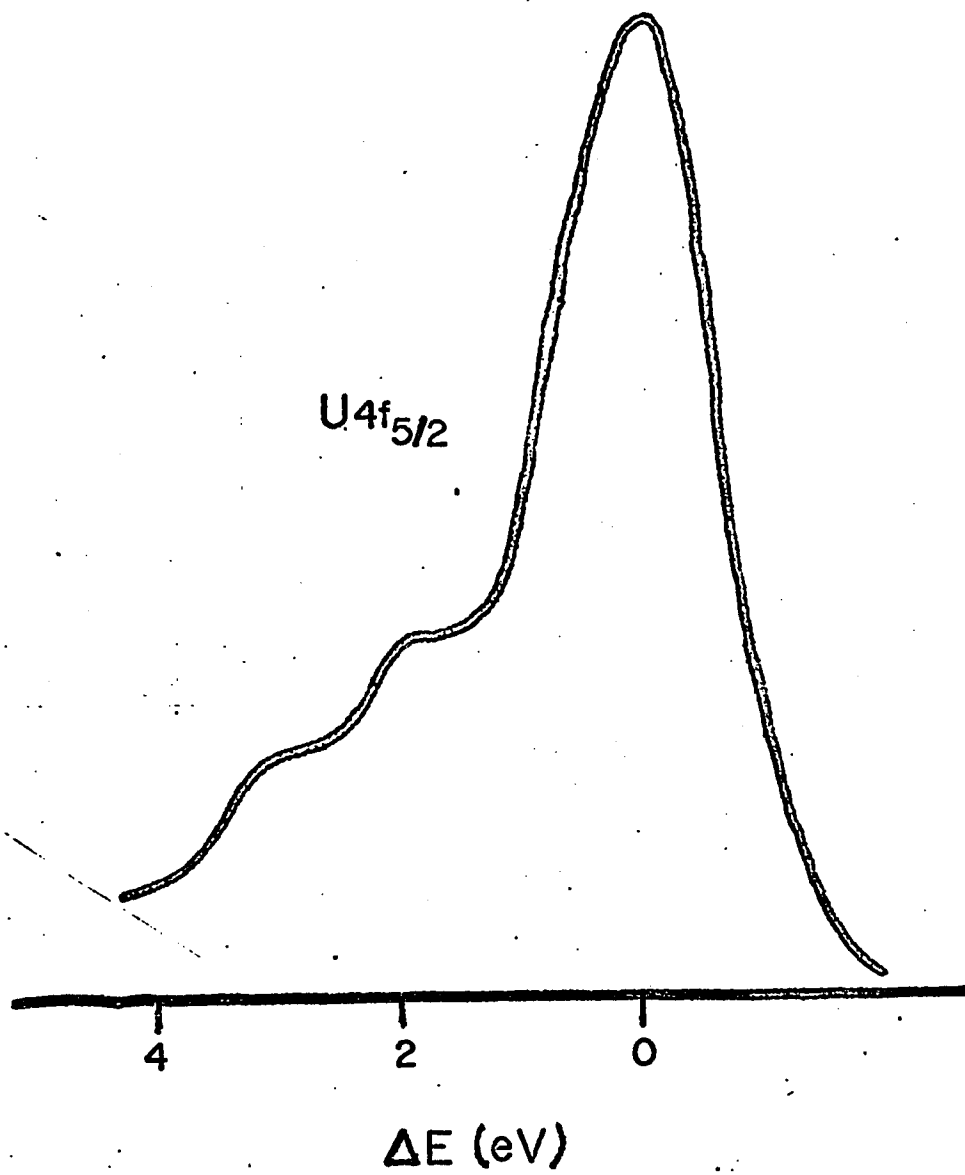


Fig. 15

References

- 1 M. O. Krause & F. Wuilleumier, *J. Phys. (B)*, 5 (1972) L143.
- 2 K. Siegbahn et al., ESCA Applied to Free Molecules, North-Holland Publishing Co., Amsterdam, 1969, Chapter 4.
- 3 D. P. Spears, H. J. Fischbeck & T. A. Carlson, *Phys. Rev. (A)*, 9 (1974) 1603.
- 4 G. K. Wertheim, R. L. Cohen, A. Rosencwaig, & H. J. Guggenheim, in Electron Spectroscopy, D. A. Shirley (ed.), North-Holland Publ. Co., Amsterdam, 1972, p. 813.
- 5 C. K. Jorgensen & H. Berthou, *Chem. Phys. Lett.*, 13 (1972) 187.
- 6 C. K. Jorgensen & H. Berthou, *Kgl. Dan. Vidensk. Selsk., Mat-Fys. Medd.*, 38 (1972) 93.
- 7 T. Aberg, *Phys. Rev.* 156 (1966) 35.
- 8 T. Aberg, *Ann. Acad. Sci. Fenn. AVI*, 308 (1969) 1.
- 9 J. S. Levinger, *Phys. Rev.*, 90 (1953) 11.
- 10 T. A. Carlson, *Phys. Rev.*, 156 (1967) 142.
- 11 T. A. Carlson, M. O. Krause, & W. E. Moddeman, *J. Phys. (Paris)* 32C4 (1971) 76.
- 12 J. A. R. Samson, *Phys. Rev. Lett.*, 22 (1969) 693.
- 13 M. O. Krause, T. A. Carlson & R. D. Dismukes, *Phys. Rev.*, 170 (1968) 37.
- 14 C. F. Fischer, *Comput. Phys. Commun.*, 1 (1969) 151.
- 15 G. W. Wertheim & A. Rosenswaig, *Phys. Rev. Lett.*, 26 (1971) 1179.
- 16 L. J. Aarons, M. F. Guest & I. H. Hillier, *J. Chem. Soc., Faraday Trans.*, 68 (1972) 1866.
- 17 U. Gelius, C. J. Allen, D. A. Allison, H. Siegbahn & K. Siegbahn, *Chem. Phys. Lett.*, 11 (1971) 224.
- 18 J. A. Pople & D. L. Beveridge, Approximate Molecular Orbital Theory, McGraw-Hill, New York, 1970.

- 19 S. Pignataro, R. DiMarino, G. Distefano & A. Mangini, Chem. Phys. Lett., 22 (1973) 352.
- 20 I. Ikemato, J. M. Thomas & H. Kuroda, J. Chem. Soc., Faraday Trans., 69 (1973) 270.
- 21 T. X. Carroll & T. D. Thomas, J. Electron Spectrosc., 4 (1974) 270.
- 22 S. Pignataro, R. DiMarino, & G. Distefano, J. Electron Spectrosc., 4 (1974) 90.
- 23 U. Gelius, C. J. Allen, G. Johansson, H. Siegbahn, D. A. Allison & K. Siegbahn, Physica Scripta, 3 (1971) 237.
- 24 J. H. D. Eland, J. Mass Spectrom. Ion Phys., 2 (1969) 471.
- 25 A. D. Baker & D. Betteridge, Photoelectron Spectroscopy, Pergamon Press, London, 1972.
- 26 H. H. Jaffe & M. Orchin, Theory and Application of Ultra-violet Spectroscopy, Wiley, New York, 1962.
- 27 L. Yin, I. Adler, T. Tsang, L. J. Matienzo & S. O. Grim, Chem. Phys. Lett., 24 (1974) 81.
- 28 A. D. Hamer, D. G. Tisley & R. A. Walton, J. Inorg. Nucl. Chem., 36 (1974) 1771.
- 29 S. Pignataro, A. Foffani & G. Distefano, Chem. Phys. Lett., 20 (1973) 350.
- 30 M. J. Tricker, J. Inorg., Nucl. Chem., 36 (1974) 1543.
- 31 L. Y. Johansson, R. Larsson, J. Blomquist, C. Cederstrom, S. Grapengiesser, U. Helgeson, L. C. Moberg and M. Sundbom, Chem. Phys. Lett., 24 (1974) 508.
- 32 M. Barber, J. A. Connor & I. H. Hillier, Chem. Phys. Lett., 9 (1971) 570.
- 33 R. Wallbank, E. C. Johnson & I. G. Main, J. Phys. Chem., 6 (1973) L340.
- 34 S. Hufner & G. L. Wertheim, Phys. Rev. B, 7 (1973) 5086.
- 35 A. Rosencwaig, G. K. Wertheim & H. J. Guggheim, Phys. Rev. Lett., 27 (1971) 479.

- 36 D. C. Frost, C. A. McDowell & I. S. Woolsey, Chem. Phys. Lett., 17 (1972) 320.
- 37 D. C. Frost, C. A. McDowell & I. S. Woolsey, Molecular Phys., 27 (1974) 1473.
- 38 T. Novakov, Phys. Rev. B, 3 (1971) 2693.
- 39 A. Rosencwaig & G. K. Wertheim, J. Electron Spectrosc., 1 (1972/73) 493.
- 40 D. C. Frost, A. Ishitani & C. A. McDowell, Molecular Phys., 24 (1972) 861.
- 41 K. S. Kim, Chem. Phys. Lett., 26 (1974) 234.
- 42 K. S. Kim & R. E. Davis, J. Electron Spectrosc., 1 (1972/73) 251.
- 43 C. A. Tolman, W. M. Riggs, W. J. Linn, C. M. King, & R. C. Wendt, Inorg. Chem., 12 (1973) 2770.
- 44 L. Matienzo, L. Yin, S. O. Grim, & W. Schwartz, Inorg. Chem., 12 (1973) 2764.
- 45 K. S. Kim, J. Electron Spectrosc., 3 (1974) 217.
- 46 M. Brisk & A. D. Baker, J. Electron Spectrosc., in print.
- 47 M. Brisk, A. D. Baker, & H. G. Britain, submitted to Inorg. Chem.
- 48 J. Escard, G. Mavel, J. E. Guerschais, & R. Kergoat, Inorg. Chem., 13 (1974) 695.
- 49 C. K. Jorgensen, Acta Chem. Scand., 11 (1957) 165.
- 50 Z. Libus, J. Inorg. Nucl. Chem., 24 (1962) 619.
- 51 S. P. McGlynn & J. K. Smith, J. Mol. Spectrosc., 6 (1961) 164.
- 52 A. F. Orchard & A. Hammett, "Electronic Structure and Magnetism of Inorg. Compounds," Specialist Periodical Reports, Vol. 3, 1973, 216.
- 53 S. Cradock & W. Duncan, Mol. Phys., 27 (1974) 837.
- 54 We have measured the satellite main peak splitting for CuCl_2 . A value of ~ 8 eV was obtained which is close to the value reported in the work of Frost et al. (Mol. Phys., 24, (1972) 861). The only type of transition possible would be of a $L6e_g \longrightarrow Mde_g$ nature.⁴ Since the satellite-

- main peak splitting for MnCl_2 is ~ 5 eV, this type of transition is unlikely to be the one that gives rise to the observed satellite peaks in the Mn(II) complexes investigated.
- 55 J. C. Carver, G. K. Schweitzer, & T. A. Carlson, *J. Chem. Phys.*, 57, (1972) 973.
- 56 M. V. Zeller & R. G. Hayes, *Chem. Phys. Lett.*, 10, (1971) 610.
- 57 As mentioned in the text tetrahedral CoCl_4^{2-} can give rise to satellites as a result of only $t_2 \longrightarrow t_2$ type transitions. The spectrum in ref. 2 shows this transition to be ~ 5 eV. Since the satellite peak in CoCl_2 appears with a satellite-main peak splitting of a little less than 5 eV (see reference 22) a $L 6 e_g \longrightarrow M d e_g$ transition would be an unlikely assignment.
- 58 C. K. Jorgensen, Absorption Spectra and Chemical Bonding in Complexes, Pergamon Press, 1962, Chapter 9.
- 59 R. L. Lintvedt & L. K. Kernitsky, *Inorg. Chem.*, 9 (1970) 491.
- 60 I. Hanazaki, F. Hanazaki, & S. Nagakura, *J. Chem. Phys.*, 50, (1969) 276.
- 61 D. W. Barnum, *J. Inorg. Nucl. Chem.*, 21 (1961) 221.
- 62 J. P. Fackler, Jr., M. L. Middleman, H. Weigold, & G. M. Barrow, *J. Phys. Chem.*, 72, (1968) 4631.
- 63 G. J. Bullen, R. Mason, & P. Pauling, *Inorg. Chem.*, 4, (1965) 456.
- 64 A. B. P. Lever, Inorganic Electron Spectroscopy, Amsterdam, 1968, Chapter 8.
- 65 D. Sutton, Electronic Spectra of Transition Metal Complexes, McGraw-Hill, London, 1968.
- 66 M. Brisk & A. D. Bakery *J. Electron Spectrosc.*, in press.

CHAPTER III

X-Ray Photoelectron Spectroscopy of Cytochrome C and of Some Copper Proteins

X-Ray Photoelectron Spectroscopy appears to be a potentially important tool to the biochemist. The technique has several aspects which are particularly amenable to biochemical substances: small amounts of material are required for analysis (\sim microgram), materials can be retrieved after analysis, and in addition air sensitive compounds can be examined since the pressure inside the target chamber is $\sim 10^{-8}$ torr. ESCA samples however must be in either a solid or gaseous state and so biochemicals are frequently examined as frozen solutions. The cryogenic probe can in general handle temperatures down to -170°C .

Previous ESCA studies of the ferridoxins¹ (non-heme proteins) and of erythrocuprein² have added to the understanding of these very important biological molecules. Because of the vital role of heme and copper proteins in physiological systems, we embarked upon an ESCA study of these substances in an effort to facilitate further understanding of their structure and function. It is interesting to note that as a result of our investigation of cytochrome c it appears that ESCA can provide information regarding structure-function relationships not only for Cytochrome systems but for such structurally related enzymes as P_{450} and P_{448} .

EXPERIMENTAL

The Hewlett-Packard 5950 ESCA model was used in this work. The horse-heart cytochrome c investigated was examined as a frozen aqueous solution by the employment of a cryogenic probe (-160°C). Approximately one hour of scanning time was used for the acquisition of each spectrum. cytochrome c was in the oxidized form (Fe(III)). A CN^- substituted cytochrome c was prepared by adding an excess of KCN to an aqueous solution of the heme protein. The cyano group is known to replace the methionine sulfur that is bound to the iron.³ This cyano-cytochrome c was also examined as a frozen aqueous solution.

The copper proteins, tyrosinase and ceruloplasmin were in the solid state. Gold plated platens were used as sample backings for these proteins as well as for the cytochromes. It should be noted that absorption spectra were obtained before and after ESCA analysis.

Results and Discussion

Cytochrome C

Cytochromes⁴ are heme proteins which participate in electron transport chains in the mitochondria in which the Fe(III)-Fe(II) redox couple is linked with the electron transfer. Cytochrome c⁵ therefore is only one component in the electron transport chain. Horse-heart cytochrome c with a molecular weight of approximately 12,400 involves 104

amino acid residues in the protein chain. The molecule contains four sulfur atoms, two of which are in thioether bridges while the other two are found in methionine residues. The protein is linked to the porphyrin via the thioether (cysteine) bridges. The axial ligands are imidazole and probably methionine. Therefore, three sulfurs are bonded to carbons only while one sulfur is bonded not only to two carbons but to the Fe as well.

Previous work on a variety of S containing compounds indicates that the S2p binding energy is approximately the same for compounds in which the S is bound to two carbons.⁶ Chemical shifts of less than 1 eV have been reported for compounds in which the S is bound to different types of carbons. However a substantial change is observed whenever oxygen, for example, is substituted for one or both carbons, or when S is bound to three or four atoms instead of two.⁶ Sulfur core electron binding energies appear to be sensitive to changes in oxidation state. In light of these reported results, one would predict a priori that the S 2p electron energy spectrum of cytochrome c would contain two resolved peaks due to the two inequivalent types of sulfurs or at least one very broad peak. As it turned out two distinct peaks were observed at 167.4 and 163.0 eV in an approximately 3:1 intensity ratio. Since ESCA is a surface technique and cytochrome c is a large molecule the peaks cannot be assigned to the two types of sulfurs by intensity considerations.

Only those sulfurs within $15 \text{ \AA}^{7,8}$ from the surface will contribute to the peak intensity. Therefore, the CN^- substituted cytochrome c was examined in order to make peak assignments. The peak which is associated with the Fe bound S should not be present in the S 2p spectrum of this complex. As expected the S 2p spectrum of the CN^- substituted cytochrome c gave rise to only one peak with a measured binding energy of 163.0 eV. The higher binding energy peak of cytochrome c was absent.

The C 1s peaks were used for calibration. This is a valid calibration procedure since the carbons from the high molecular weight proteins contribute to essentially all of the peak intensity and these carbons should be unaffected for all practical purposes by the groups bound to the Fe. Carbon contamination is negligible due to the oil free pumping system (ion pumps) in the H. P. Spectrometer. As further evidence to support the assignment of the lower energy peak to the unbound sulfurs, we compared the binding energy of this peak to that of the S 2p band of free methionine. The binding energies were within experimental error of each other (.3 eV).

It is interesting to note that the Fe 2p spectrum of cytochrome c exhibited pronounced asymmetric character as well as a satellite band 5.4 eV from the $2p_{3/2}$ main peak. This extra peak is due to an electron shake-up process involving either a S or porphyrin π type electron being excited

to a Fe(III) d orbital. The asymmetric character of course is due to the presence of unpaired electron spin density on the metal ion.

Our results coincide with other experimental data, e.g. x-ray diffraction which imply that a methionine S is bound to Fe in the molecule.⁴ Even more importantly, it is apparent from our results that the ESCA technique can determine the integrity of this Fe-S bond which is thought to play a critical role in the physiological function of cytochrome c and of structurally similar substances. Therefore, any technique which is sensitive only to the disposition of the Fe-S bond can be applied to studies in which the effects of various denaturants and structure perturbants are determined. From such studies, it is hoped that structure-function relationships can be derived. In addition, P₄₅₀,⁹ an enzyme produced in the liver as a part of a natural detoxification system is known to have a similar structure to cytochrome c. It is thought that the Fe-S bond is cleaved during the detoxification process. The application of ESCA to this problem should support or negate this theory. In conclusion, it should be noted that Fe-S bonds are prevalent in many biologically important heme proteins and therefore any technique that can determine the status of this bond may make a significant contribution to the understanding of these molecules.

Copper Proteins

The oxidation state of copper in a protein cannot always be determined without great difficulty. EPR, magnetic susceptibility measurements, and even absorption spectroscopy cannot always distinguish between Cu(I) and Cu(II). In fact it appears that a major problem in Cu protein studies is the assignment of formal oxidation state. X-ray photoelectron studies of copper complexes have shown that the technique can readily distinguish between the oxidation states. Frost et al.¹⁰ have shown that satellite peaks do not occur in Cu(I) complexes while they have been observed in all Cu(II) compounds examined so far. As mentioned in Chapter 2, the positions and intensities of these extra peaks are functions of the ligands and of the geometry of the complex.

Tyrosinase (polyphenoloxidase) is known to catalyze the formation of the melanin pigments which, for example, give color to the skin and eyes of animals.⁴ The enzyme has four copper atoms per molecule. The oxidation state has not been definitely determined but recent work indicates that it is most probably Cu(II).¹¹ The Cu 2p spectrum of tyrosinase indicates the presence of Cu(II) only since an intense satellite band appears at 2.0 eV to the higher binding energy side of the $2p_{3/2}$ main peak. In addition, the half-width of the peak is 2.0 eV--a value which according to previous work¹⁰ also points to the presence of divalent

copper. Cu(II) core electron peaks are in general broader than the corresponding Cu(I) bands because of multiplet splitting arising from the presence of unpaired electron spin density around the copper ion. It is also interesting to note that the main peak satellite splitting observed is less than all other splittings reported for divalent complexes. We have not investigated the significance of this as yet but it must be related to the high redox potential associated with this enzyme.

The exact physiological role of ceruloplasmin is not known, although it has been shown to have significant oxidase activity, and catalyzes the oxidation of Fe(II) to Fe(III).⁴ It has been suggested that this copper protein incorporates iron into the protein part of transferrin (apotransferrin) and consequently facilitates hemoglobin formation. It is interesting to note that Wilson's disease in which copper concentrations are 100 times greater than normal, is associated with a deficiency of ceruloplasmin.

Ceruloplasmin has a molecular weight of 155,000 containing 8 copper atoms per molecule. EPR and magnetic susceptibility measurements imply that 40-44% of the copper is divalent.¹² The Cu 2p spectrum of this enzyme however indicated the presence of Cu(I) only. Two narrow 2p peaks appear in which the $2p_{3/2}$ band has a halfwidth of 1.2 eV. The discrepancy between the experimental results may be caused by Cu(I) ions being near the surface of the protein while the Cu(II) ions

are embedded within the molecule so that the photoejected Cu(II) electrons cannot be detected. If this is the case then if the protein is denatured, i.e. a homogeneous sample is formed since the protein structure is destroyed, Cu(II) 2p electron peaks should appear in the ESCA spectrum as well.

References

- 1 L. N. Kramer & M. P. Klein in Electron Spectroscopy, D. A. Shirley (ed.), 1972, p. 733, North-Holland Publishing Co., Amsterdam.
- 2 G. Jung, M. Ottnad, W. Bohenkamp & U. Weser, Febs. Lett., 25 (1972) 346.
- 3 G. L. Eichhorn, Inorganic Biochemistry, Elsevier Scientific Publishing Co., Amsterdam, 1973, Chapter 26.
- 4 M. N. Hughes, The Inorganic Chemistry of Biological Processes, Wiley, London, 1972, Chapter 5.
- 5 E. Margoliash & A. Scheztor, Adv. Protein Chem., 21 (1966) 113.
- 6 A. D. Baker & D. Betteridge, Photoelectron Spectroscopy, Pergamon Press, Oxford, 1972, Chapter 6.
- 7 G. A. Katrick & O. G. Sarber, Sov. Phys. Solid State, 3 (1961) 1181.
- 8 I. Lindau & W. E. Spicer, J. Electron Spectrosc., 3 (1974) 409.
- 9 T. Omura & R. Soto, J. Biol. Chem., 239 (1964) 2370.
- 10 D. C. Frost, A. Ishitani, & C. A. McDowell, Mol. Phys., 24 (1972) 861.
- 11 N. Makino, P. McMahon, & H. S. Mason, J. Bio. Chem., 249 (1974) 6062.
- 12 I. H. Scheinberg in The Biochemistry of Copper, J. Peisach, P. Arsin & U. E. Blumber, (eds.), 1966, p. 513, Academic Press, New York.

CHAPTER IV

Photoelectron Spectra and Dihedral Angles of Disulfides

Previous papers noting the dependence of photoelectron spectra on the dihedral angle in biphenyls,¹ and substituted anilines,² prompt us to report briefly on similar studies with disulfides and related compounds.⁹

Disulfides, peroxides, diselenides, and ditellurides represent an ideal and somewhat unique series for studying the interactions between p-orbitals on adjacent atoms as the geometry and general characteristics of the system are changed.

For such molecules, the first two bands in the photoelectron spectra correspond to the symmetric and anti-symmetric combinations of the outermost p-atomic orbitals, producing orbitals $p\pi$ and $p\pi^*$ respectively. In general it is to be expected that as the dihedral angle deviates from 90° , the energy separation ΔE between the $p\pi$ and $p\pi^*$ orbitals will increase.

A relationship between ΔE and θ for disulfides is given by Bergson's equation:³

$$\Delta E = \frac{2\gamma/\cos \theta}{1 - (0.129/\cos \theta)^2}$$

where γ is empirically determined from ultraviolet absorption.⁴

Literature values of θ for disulfides differ,^{5,6} and thus we thought it instructive to measure the $3p\pi$ and $3p\pi^*$ ionization potentials through photoelectron spectroscopy, and use the Δ IP value to calculate θ .

Measured ionization potentials for dimethyl, diethyl, and di-*t*-butyl disulfides are given in Table 4.1, whilst the calculated dihedral angles are given in Table 4.2, along with other previously reported values. It is evident that our values reported by Sutter et al.⁶

Table 4.1
 Ionization Potentials (eV) for Dimethyl,
 Diethyl and Di-t-butyl Sulfides

		Measured vertical IPs			Other values (first adiabatic IP only)	
		Me ₂ S ₂	Et ₂ S ₂	t-Bu ₂ S ₂	Me ₂ S ₂ (ref.)	Et ₂ S ₂ (ref.)
3p	*	8.98	8.85	8.20	8.46(7)	8.27(7)
3p		9.28	9.10	8.85		

Table 4.2
 Dihedral Angles (degrees) for Dimethyl,
 Diethyl and Di-t-butyl Disulfides

	Me ₂ S ₂ (ref.)	Et ₂ S ₂ (ref.)	t-Bu ₂ S ₂ (ref.)
Literature values	68 (5)	74 (5)	83 (5)
Our calculated values	84.7 (6)	84.7 ^a	96.4 (4,8)
	85.5 ± 0.5 ^b	84.5 ± 0.5 ^b	97.5 ± 0.5 ^b

a Value used by Nelander⁴ in his charge transfer work. He assumed the dihedral angle in Et₂S₂ is the same as the dihedral angle in Me₂S₂.

b Angles could only be determined within approximately a 1° range because of the number of significant figures in the values of γ taken from the literature.

References

- 1 J. P. Maier & D. W. Turner, Discuss, Faraday Soc., 54, (1972) 149.
See also, J. Daintith, J. P. Maier, D. A. Sweigart & D. W. Turner, in D. A. Shirley (ed.), Electron Spectroscopy, North-Holland Publ. Co., Amsterdam, 1972, pp. 289-310.
- 2 S. A. Cowling & R. A. W. Johnstone, J. Electron Spectrosc., 2 (1973) 161.
- 3 G. Bergson, Ark. Kem, 12 (1958) 233.
- 4 B. Nelander, Acta Chem. Scand., 23 (1969) 2127.
- 5 C. W. N. Cumper, J. Read & A. I. Vogel, J. Chem. Soc., 5323, 1965.
- 6 D. Sutter, H. Dreizler & H. D. Rudolph, Z. Naturforsch., 20a (1965) 1676.
- 7 K. Watanabe, T. Nakayama & J. Mottl, Final Report on Ionization Potential of Molecules by a Photoionization Method. Dec. 1959. Dept. of Army No. 5B99-01-004 ORD-TB2-0001-00R-1624, Contract No. DA-04-200-ORD 480 & 737.
- 8 M. Rogers & T. Campbell, J. Amer. Chem. Soc., 74 (1952) 4742.
- 9 A. D. Baker, M. Brisk and M. Gellender, J. Electron Spectrosc, 3 (1974) 227.